

PHYSIOLOGY

Circulating fructose regulates a germline stem cell increase via gustatory receptor–mediated gut hormone secretion in mated *Drosophila*

Ryo Hoshino¹, Hiroko Sano², Yuto Yoshinari^{3,4}, Takashi Nishimura³, Ryusuke Niwa^{4*}

Oogenesis is influenced by multiple environmental factors. In the fruit fly, *Drosophila melanogaster*, nutrition and mating have large impacts on an increase in female germline stem cells (GSCs). However, it is unclear whether these two factors affect this GSC increase interdependently. Here, we report that dietary sugars are crucial for the GSC increase after mating. Dietary glucose is required for mating-induced release of neuropeptide F (NPF) from enteroendocrine cells (EECs), followed by NPF-mediated enhancement of GSC niche signaling. Unexpectedly, dietary glucose does not directly act on NPF-positive EECs. Rather, it contributes to elevation of hemolymph fructose generated through the polyol pathway. Elevated fructose stimulates the fructose-specific gustatory receptor, Gr43a, in NPF-positive EECs, leading to NPF secretion. This study demonstrates that circulating fructose, derived from dietary sugars, is a prerequisite for the GSC increase that leads to enhancement of egg production after mating.

INTRODUCTION

Oogenesis is modulated by multiple, environmental stimuli in organisms ranging from invertebrates to mammals. For example, oogenesis is greatly influenced by nutrient availability, as oocytes require large amounts of energy to ensure production of mature eggs (1). In particular, insect oogenesis is typically nutrient-dependent and is severely suppressed when sufficient nutrients are unavailable (2). In addition, insect oogenesis is also affected by mating stimuli that accelerate egg production (3). It is thought that the nutrient and mating dependencies of insect oogenesis are an adaptive phenomenon, as female insects generally need to lay large numbers of large eggs after mating, despite small body sizes.

To discover mechanisms that have evolved to tightly couple oogenesis to nutrient availability and mating stimuli, the fruit fly, *Drosophila melanogaster*, serves as an excellent model (1, 4). In *D. melanogaster*, a mated adult female lays approximately 40 to 60 eggs per day under favorable nutritional conditions, which is equivalent to 30 to 50% of its body weight. Because oogenesis is such an energy-intensive process, even a few days of poor nutrition slow division of germline stem cells (GSCs) and cyst cells, suppressing vitellogenesis (1, 4). Mating also accelerates multiple steps of oogenesis, including the increase in GSC numbers (5, 6). Moreover, female feeding behavior is related to mating, which enhances food intake to ensure allocation of energy for egg production in *D. melanogaster* (7, 8).

Regarding the relationship between nutrition and egg formation in *D. melanogaster*, most studies have focused on protein, because dietary protein has a major impact on oogenesis (4, 9, 10). Previous studies have reported that nutritional conditions without dietary

protein retard the mitotic rate and induce cell death in ovarian somatic cells and multistage germline cells, including GSCs (11). Under protein-rich conditions, *Drosophila* insulin-like peptides (DILPs) and the insulin receptor are activated, resulting in GSC maintenance and acceleration of oogenesis. Conversely, protein-poor conditions suppress DILP signaling, GSC mitosis, and vitellogenesis and enhance ovarian somatic cell death (4, 12). More recent studies have demonstrated that other diet-related signaling pathways, such as target of rapamycin, adenosine monophosphate–dependent protein kinase, and adiponectin signaling, regulate many aspects of oogenesis for an adaptive response to protein-rich protein or protein-poor diets (4).

On the other hand, these flies consume not only proteins from yeast growing on fruits but also many other nutrients, including dietary sugars. In addition, about 65% of the carbon in the germline is derived from sugars (13). However, few studies have examined whether dietary sugars are required for oogenesis. Very recent studies have shed light on the effect of dietary sugars on germline development in *D. melanogaster* (14, 15). Similar to the effect of amino acid deprivation, deprivation of dietary carbohydrates for females reduces ovary size, compared to normal carbohydrate feeding, leading to a drastic decrease in the number of eggs laid. In addition, another study has shown that enzymes regulating glucose consumption and cytosolic acetyl–coenzyme A production in adipocytes promote early germline cyst survival (16). These results imply that dietary carbohydrates and their metabolism are crucial to maintain a high level of egg production. However, compared to protein-dependent regulation of oogenesis, the influence of dietary sugars on oogenesis is still little known.

Here, we report a neuroendocrine mechanism by which dietary sugars notably influence an increase in GSCs after mating in female *D. melanogaster*. We have previously reported that a mating-induced GSC increase requires the action of multiple neuroendocrine humoral factors (6), including the midgut enteroendocrine cell (EEC)–derived, neuropeptide F (NPF) (17). In this study, we found that the NPF-dependent increase in GSCs after mating requires dietary sugars. We also revealed that hemolymph fructose,

Copyright © 2023 The Authors, some rights reserved; exclusive licensee American Association for the Advancement of Science. No claim to original U.S. Government Works. Distributed under a Creative Commons Attribution NonCommercial License 4.0 (CC BY-NC).

¹Degree Programs in Life and Earth Sciences, Graduate School of Science and Technology, University of Tsukuba, Tennodai 1-1-1, Tsukuba, Ibaraki 305-8572, Japan.

²Department of Molecular Genetics, Institute of Life Science, Kurume University, Kurume, Fukuoka 830-0011, Japan. ³Institute for Molecular and Cellular Regulation, Gunma University, 3-39-15 Showa-machi, Maebashi 371-8512, Japan. ⁴Life Science Center for Survival Dynamics, Tsukuba Advanced Research Alliance (TARA), University of Tsukuba, Tennodai 1-1-1, Tsukuba, Ibaraki 305-8577, Japan.

*Corresponding author. Email: ryusuke-niwa@tara.tsukuba.ac.jp

generated from dietary glucose through a metabolic pathway called the polyol pathway, stimulates the fructose-specific gustatory receptor (Gr) in *NPF*-positive EECs (*NPF*⁺ EECs), leading to NPF secretion. This study is the first to report that dietary sugars are important for the GSC increase through interorgan communication.

RESULTS

A mating-induced increase in female GSCs is impaired under yeast dietary conditions

To investigate the effect of nutritional status on the mating-induced GSC increase, we first compared the number of GSCs before and after mating in flies fed diets with different nutrient compositions. A standard diet in this study was a mixture of dry yeast, cornmeal, glucose, and agar (Fig. 1A and table S1; see also Materials and Methods). Along with the standard diet, we prepared five alternative diets: dry yeast with agar (yeast diet), glucose with agar (glucose diet), cornmeal with agar (cornmeal diet), dry yeast and glucose with agar [yeast-glucose (YG) diet], and dry yeast and cornmeal with agar [yeast-cornmeal (YC) diet; Fig. 1A].

The protocol of feeding experiments is illustrated in Fig. 1B. We reared wild-type flies on standard diets from eggs to young adults. Young virgin females, which we collected 5 days after eclosion, were transferred into a vial containing the standard diet and the five alternative diets. Five days after the transfer, some of these flies were then allowed to mate with males for 1 day, and other virgin flies were continuously reared without males for 1 day. We found that mating induced a GSC increase in females reared on the standard diet, as previously described (5), as well as those on the glucose, cornmeal, YG, and YC diets (Fig. 1C). In contrast, the mating-induced GSC increase was impaired in females reared on the yeast diet.

We next examined how many days after the transfer to the yeast diet the impairment of mating-induced GSC increase appeared. Young virgin females were reared on the standard diet or yeast diet for 1 to 7 days. Females from each experimental batch were reared with or without males for an additional 1 day. On the standard diet, the mating-induced GSC increase was observed at any time point examined (Fig. 1D). In contrast, on the yeast diet, the mating-induced GSC increase was observed during the first 5 days but not 6 days after the transfer (Fig. 1D).

To rule out the possibility that females on the yeast diet did not mate effectively with males, we used *dj-GFP* males in which sperm were visualized with green fluorescence (18) and examined whether sperm were successfully transferred into females on the yeast diet. We reared wild-type females on the yeast diet for 5 days. We then place females with *dj-GFP* males for 1 day. We found that more than 90% of the females carried green fluorescent sperm in their abdomens (fig. S1, A and B). This mating frequency did not differ from that of females reared on the standard diet for 6 days (fig. S1B). These results suggest that impairment of the mating-induced GSC increase on the yeast diet is not due to a failure of mating.

We next measured the amount of phosphorylated Mother against dpp (pMad) in GSCs. When the niche signal Decapentaplegic (Dpp), which is required for GSC proliferation and maintenance, is transmitted from cap cells to GSCs, it promotes phosphorylation of Mad to maintain stemness in GSCs (4). In addition, pMad intensity in GSCs is elevated in mated females,

compared to virgin females (5, 17, 19). We found that mating-induced pMad elevation was suppressed by the yeast diet, whereas the pMad level of GSCs in virgin females was unchanged between the standard and yeast diets (Fig. 1, E and F). These results suggest that impairment of the mating-induced GSC increase of flies on the yeast diet is due to impairment of mating-induced pMad elevation in GSCs.

Mating-induced NPF secretion from EECs is impaired by a yeast diet

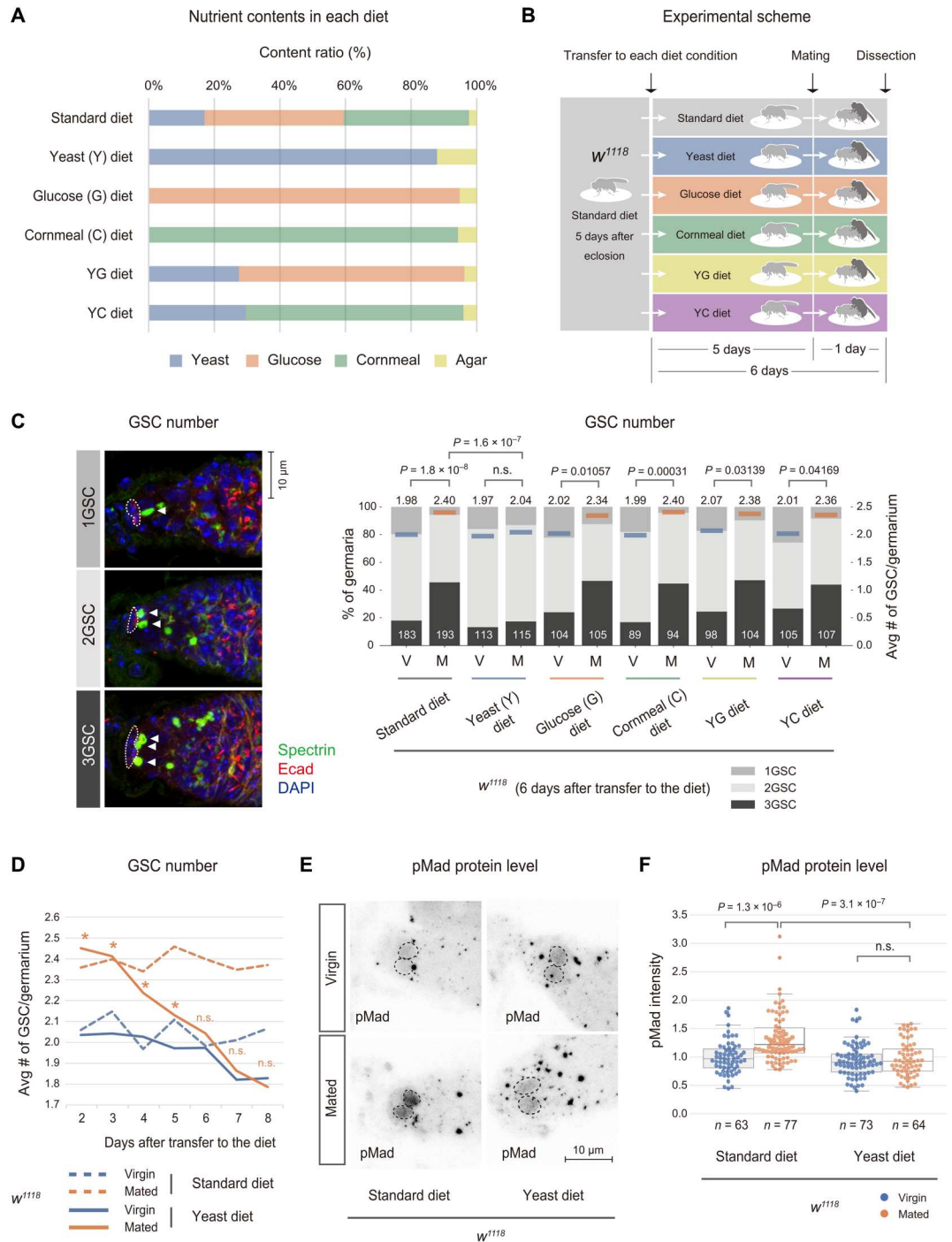
The mating-induced GSC increase requires NPF, which is released from midgut EECs upon mating and is received by ovarian somatic cells (17). Therefore, we hypothesized that impairment of this GSC increase by the yeast diet was due to suppression of the release of enteroendocrine NPF. To test this hypothesis, we first examined the amount of NPF protein in midgut EECs of wild-type virgin and mated female flies on the standard and yeast diets. On the standard diet, enteroendocrine NPF protein level was decreased in the EECs of mated females compared with virgin females (Fig. 2, A and B). However, there was no change in *NPF* mRNA abundance in the guts between virgin and mated females (Fig. 2C). As reported in our previous study (17), the high accumulation of NPF protein without *NPF* mRNA increase indicates a failure of NPF secretion from EECs. On the other hand, on the yeast diet, NPF protein levels were not changed between virgin and mated females (Fig. 2, A and B). On the yeast diet, while *NPF* mRNA levels increased in both virgin and mated females, mating did not induce an increase in the *NPF* mRNA level in the guts (Fig. 2C). These results suggest that NPF release from midgut EECs is suppressed by the yeast diet, even after mating.

On the basis of these results, we expected that the failure of the mating-induced GSC increase on the yeast diet would be rescued by enhancing the level of circulating NPF. Therefore, we manually delivered synthetic NPF peptide by injecting it into adult females using glass needles. As we previously reported (5), NPF injection into wild-type females on the standard diet resulted in an increase in GSC number compared with injection of phosphate-buffered saline (PBS) into virgin females (Fig. 2D). NPF injection into wild-type females on the yeast diet also induced an increase in GSC numbers, regardless of whether they were virgin or mated females (Fig. 2D). Consistent with these results, NPF injection-induced GSC increases were strongly associated with an elevation of pMad intensity in GSCs, in both virgin and mated females (Fig. 2, E and F, and fig. S2, A and B). *TKg-GAL4*-mediated overexpression of *NPF* in *NPF*⁺ EECs did not fully restore the failure of the mating-induced GSC increase on the yeast diet (fig. S2C), indicating that NPF release is gated by the yeast diet. Therefore, these results suggest that NPF release from midgut EECs after mating is suppressed by the yeast diet, leading to impairment of a mating-induced GSC increase through Dpp niche signaling.

Dietary sugar is necessary and sufficient for an increase in mating-induced GSCs

The results described above imply that nutritional differences between the yeast diet and other diets must account for the difference in the mating-induced GSC increase, which is mediated by enteroendocrine NPF. We recently reported that the release of NPF from EECs is stimulated by dietary sugar in virgin females (20). A liquid chromatography–mass spectrometric analysis revealed that

Fig. 1. The mating-induced increase in female GSCs is impaired in wild-type flies reared on a yeast diet. (A) Proportions of raw materials in each of the diets, calculated by dry weights. Also, see table S1. (B) A schematic representation of the protocol of feeding experiments. (C) Left: Representative images of anti-spectrin (green) and anti-E-cadherin (red) immunostaining with 4',6-diamidino-2-phenylindole (DAPI) staining (blue). Top, middle, and bottom images represent one, two, and three GSCs, respectively. Arrowheads and dashed circles indicate the positions of GSCs and cap cells, respectively. Right: Frequencies of germaria containing one, two, and three GSCs (left vertical axis) and the average number of GSCs per gerarium (orange and blue horizontal lines, corresponding to the right vertical axis) in wild-type (*w¹¹¹⁸*) virgin (V) and mated (M) female flies on different diet conditions. Orange and blue horizontal lines indicate more and fewer than 2.25 GSCs, respectively. Numbers in bars indicate numbers of germaria that we observed. (D) Temporal changes in GSC numbers of virgin and mated wild-type female flies on the standard diet and yeast diets. Young virgin females were reared on the standard diet or yeast diet for 1 to 7 days. Females from each experimental batch were reared with or without males for an additional 1 day. **P* < 0.05. (E) Representative images of wild-type adult female gerarium immunostained with anti-pMad antibody. GSCs are outlined with dashed lines. Flies were prepared in the same way as shown in (B). Scale bar, 10 μm. (F) Quantification of pMad intensity levels in the GSCs in virgin and mated wild-type females. Box-and-whisker plots are also represented. Statistical analysis: Wilcoxon rank sum test with Holm's correction for (C) and (F) and Wilcoxon rank sum test for (D). n.s. (not significant), *P* > 0.1.

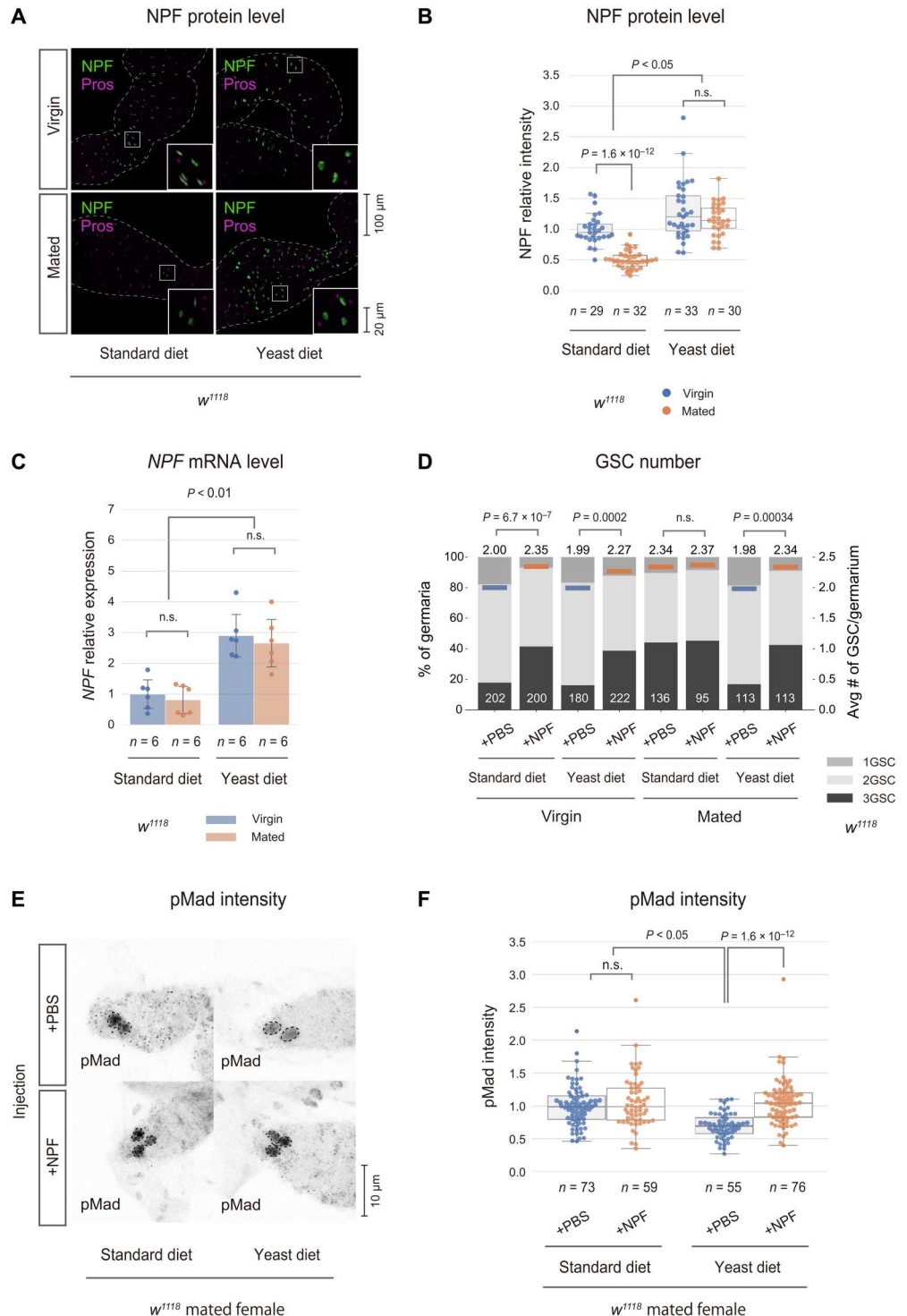


there was less glucose in hydrolysates of yeast diets than in those of the standard, glucose, cornmeal, YG, and YC diets (Fig. 3A). Therefore, we next clarified whether impairment of the mating-induced GSC increase and mating-induced enteroendocrine NPF secretion on the yeast diet was due to a lack of dietary sugars.

The protocol of feeding experiments is illustrated in Fig. 3B. We first investigated the effect of dietary sugar on the mating-induced GSC increase. We reared wild-type flies on both standard and yeast diets. Then, we transferred these flies to the standard diet, yeast diet,

or a diet containing sucrose with agar (sucrose diet), followed by a 5-day culture period after the transfer. Some of these flies were then allowed to mate with males for 1 day, and other virgin flies were continuously reared without males for 1 day. After mating, GSCs increased in flies raised on all diets, even those that were reared on the yeast diet beforehand (Fig. 3C). Considering that glucose and sucrose diets contain only glucose and sucrose, respectively, as major nutrients, these results suggest that dietary sugar is necessary and sufficient for the mating-induced GSC increase.

Fig. 2. Mating-induced NPF release from the midgut and the subsequent pMad elevation in GSCs are impaired in flies on the yeast diet. Wild-type (w^{1118}) flies reared on different diets were prepared as shown in Fig. 1B. (A to C) Levels of NPF protein and NPF mRNA in the middle midgut of wild-type females. (A) Representative images of anti-NPF (green) and anti-Prospero (Pros) (pan-EEC marker; magenta) immunostaining in the middle midgut. Scale bar, 100 μ m. (B) Quantification of anti-NPF signal intensity in NPF^+ EECs. Box-and-whisker plots are also represented. (C) The abundance of NPF mRNA in the gut did not change after mating in either standard or yeast diets, as determined by quantitative reverse transcription polymerase chain reaction (RT-qPCR). (D to F) Effect of NPF injection into wild-type females reared on standard and yeast diets. (D) Frequencies of germaria containing one, two, and three GSCs (left vertical axis) and the average number of GSCs per germarium (orange and blue horizontal lines in the bar graphs, corresponding to the right vertical axis) in wild-type virgin and mated females injected with PBS (control) and synthetic NPF peptides. Orange and blue horizontal lines indicate more and fewer than 2.25 GSCs, respectively. Numbers in bars indicate numbers of germaria that we observed. (E) Representative images of anti-pMad immunostaining in germaria of wild-type mated female reared on standard or yeast diets with or without NPF injection. GSCs are outlined with dotted lines. Scale bar, 10 μ m. (F) Quantification of pMad intensity levels in GSCs of wild-type mated females reared on standard and yeast diets with or without NPF injection. Box-and-whisker plots are also represented. Statistical analysis: Wilcoxon rank sum test with Holm's correction for (B), (D), and (F); and Tukey-Kramer's HSD test for (C). n.s., $P > 0.1$.



We next measured enteroendocrine NPF protein levels in wild-type flies that were initially fed the yeast diet followed by a transfer to the standard, glucose, or sucrose diet using the same experimental protocol as shown in Fig. 3B. We found that NPF protein accumulation in EECs was reduced after mating in flies administered the standard, glucose, or sucrose diet following the yeast diet (Fig. 3,

D and E). These results suggest that dietary sugar is also necessary and sufficient for mating-induced NPF release from EECs.

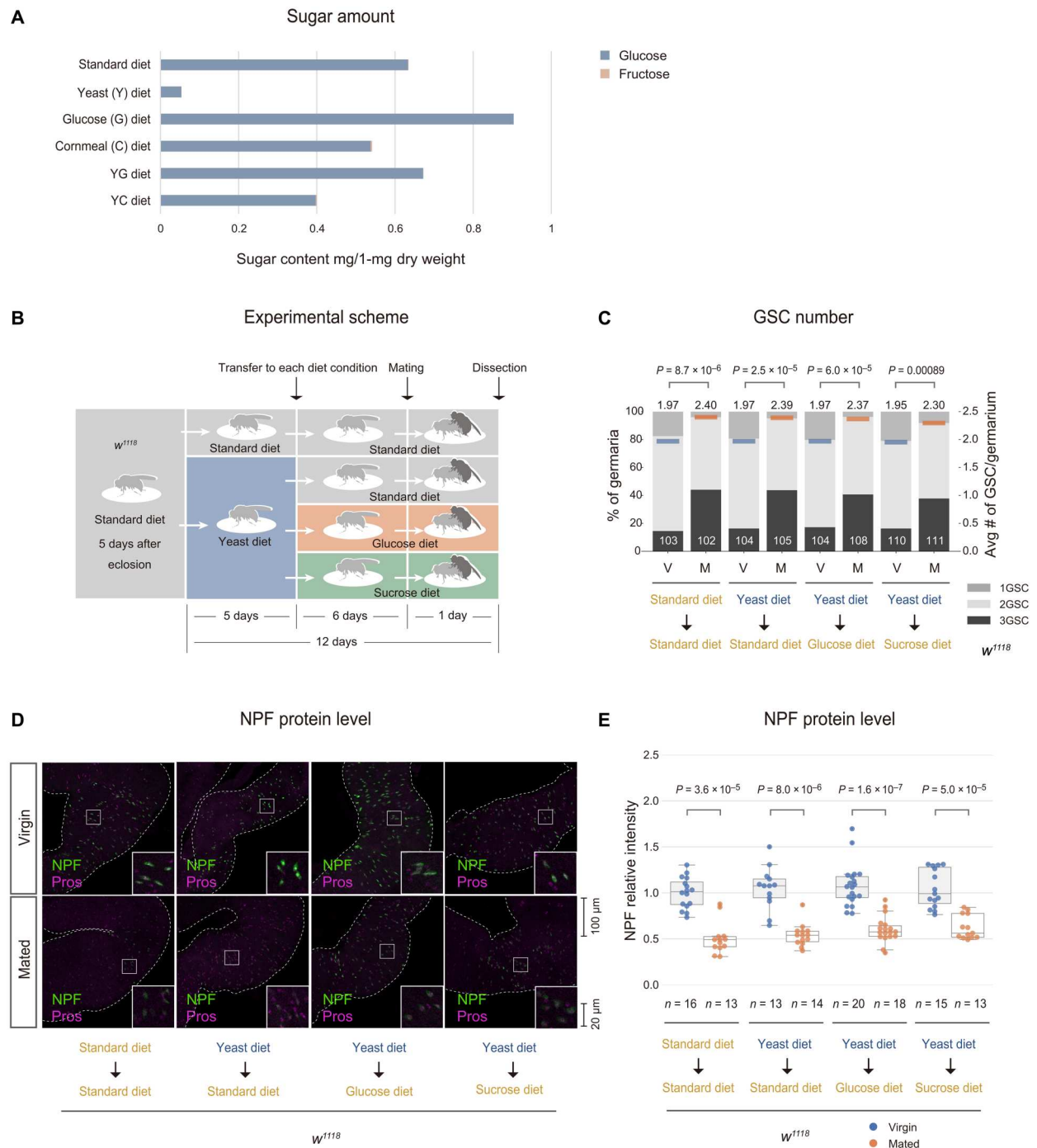


Fig. 3. Sugar is indispensable for the GSC increase and the enteroendocrine NPF release after mating. (A) Estimated amounts of glucose and fructose in diets used in this study. To measure glucose amounts, each diet material was hydrolyzed with amyloglucosidase. See Materials and Methods for details. Raw data are described in table S1. (B) Schematic representation of the protocol of feeding experiments. Newly eclosed, wild-type virgin females were first reared on the standard diet for 5 days. Then, these flies were transferred to the standard diet or yeast diet for 6 days. Subsequently, these flies were transferred to the standard diet, glucose diet, or sucrose diet and then reared for 5 days. Last, these females were placed with or without males for 1 day. Note that, when wild-type flies were continuously fed the yeast diet for 11 days, these flies did not survive. Therefore, we do not include those data in this figure. (C) Frequencies of germaria containing one, two, and three GSCs (left vertical axis) and the average number of GSCs per germarium (orange and blue horizontal lines, corresponding to the right vertical axis) in wild-type (w^{1118}) virgin and mated females reared on different diets. Orange and blue vertical lines indicate more and less than 2.25 GSCs, respectively. Numbers in bars indicate numbers of germaria that we observed. (D and E) Levels of NPF protein in the middle midgut of wild-type females, which were prepared as shown in (C). (D) Representative images of anti-NPF (green) and anti-Pros (pan-EEC marker; magenta) immunostaining in NPF^+ EECs. (E) Quantification of anti-NPF signal intensity in NPF^+ EECs. Box-and-whisker plots are also represented. Statistical analysis for (C) and (E): Wilcoxon rank sum test with Holm's correction.

Dietary sugar-dependent NPF release after mating is regulated via the fructose receptor, Gr43a, present in NPF-positive EECs

Our previous study demonstrated that sugar-responsive NPF release from midgut EECs in virgin females requires the low-affinity glucose transporter solute carrier family 2 (SLC2) protein, Sugar transporter1 (Sut1) (20). Therefore, we initially expected that Sut1 must also be necessary for mating-induced NPF release from EECs. However, unexpectedly, in females of *Sut1* RNA interference (RNAi) driven by *Tkg-GAL4*, which is active in *NPF*⁺ EECs (17, 20, 21), we found that the NPF protein level in EECs was still reduced after mating in flies on the standard diet (fig. S3, A and B). In addition, on the standard diet, the mating-induced GSC increase was observed in *Tkg-GAL4*-driven *Sut1* RNAi females (fig. S3C). These results suggest that Sut1 does not make a major contribution to NPF release from EECs after mating.

To clarify the mechanism of the sugar-responsive NPF release after mating, we focused on Grs responsible for sugar detection. In mammals, some Grs present in EECs receive nutrients and regulate enteroendocrine hormone release in response to nutrients (22, 23). In *D. melanogaster*, some *Gr* genes are expressed in *NPF*⁺ EECs (24), although their function in EECs has not been determined. We first conducted a transgenic RNAi experiment to examine which *Gr* in EECs is involved in the mating-induced GSC increase. We knocked down each of 13 *Gr* genes using *R46G06-GAL4*, reportedly active in *NPF*⁺ EECs (17). Of the 13 Grs, 7 are reportedly expressed in EECs (24), while 9 have been characterized as sugar taste receptors (25, 26). We found that RNAi of genes encoding bitter taste receptors (Gr28b, Gr33a, Gr36c, and Gr93a) (27) and some sugar taste receptors (Gr61a, Gr64b, Gr64c, Gr64d, and Gr64e) had no effects on the mating-induced GSC increase (fig. S4A). In the case of RNAi of *Gr64a*, encoding a sugar taste receptor, GSC numbers in virgin females were abnormally high (fig. S4A). Therefore, we could not fairly evaluate the function of *Gr64a* in this study. In contrast, RNAi of genes encoding three sugar taste receptors, Gr5a, Gr43a, and Gr64f, impaired the mating-induced GSC increase (fig. S4A). Gr5a and Gr43a are taste receptors for sensing trehalose and fructose, respectively, while Gr64f can sense multiple sugars, including glucose and sucrose (26, 28, 29).

We next examined whether *Gr5a*, *Gr43a*, *Gr64a*, and *Gr64f* are expressed in *NPF*⁺ EECs using *GAL4* transgenes fused with the promoters of these *Gr* genes. Consistent with a previous study (24), *Gr43a-GAL4* expression was observed in approximately 70% of *NPF*⁺ EECs (Fig. 4A), while we did not observe any obvious expression of *Gr5a-GAL4*, *Gr64a-GAL4*, or *Gr64f-GAL4* in *NPF*⁺ EECs (fig. S4, B to D). *Gr43a* expression is also supported by a single-cell RNA sequencing database of EECs (30). Therefore, we decided to focus on Gr43a for further analyses in this study.

NPF protein level was not reduced after mating in *R46G06-GAL4*-driven *Gr43a* RNAi animals without a change in the gut *NPF* mRNA level between virgin and mated females (fig. S5, A to C). We also used a genetic approach to examine the function of Gr43a in the mating-induced NPF release from EECs. As with *R46G06-GAL4*-driven *Gr43a* RNAi, neither NPF protein levels in EECs nor *NPF* mRNA levels in the gut were reduced after mating in *Gr43a* genetic loss-of-function mutant females (fig. S5, D to F). Moreover, the mating-induced GSC increase was also impaired by a *Gr43a* genetic loss-of-function mutation (fig. S5G). Under our experimental conditions, there were no differences in food

consumption between control and *Gr43a* genetic loss-of-function mutants (fig. S5H), suggesting that GSC phenotypes are not a secondary effect of malnutrition.

We realized that *R46G06-GAL4* was active not only in *NPF*⁺ EECs (17) but also in adult peripheral sensory organs, including proboscises, legs, and ovipositors (fig. S6, A to C) where *Gr43a* is expressed (29). To rule out the possibility that impairment of enteroendocrine NPF release and the mating-induced GSC increase was due to Gr43a function in peripheral sensory organs, we also used *Tkg-GAL4* that was inactive in these tissues (fig. S6, D to F). We confirmed that NPF protein levels were not reduced after mating of *Tkg-GAL4*-driven *Gr43a* RNAi females without a change in gut *NPF* mRNA levels between virgin and mated females (Fig. 4, B to D). These results suggest that release of enteroendocrine NPF is suppressed when Gr43a function is inhibited in EECs. We also confirmed that mating frequency did not differ between control and *Tkg-GAL4*-driven *Gr43a* RNAi animals (fig. S7A), suggesting that impairment of the NPF release in loss-of-*Gr43a*-function animals is not due to mating failure.

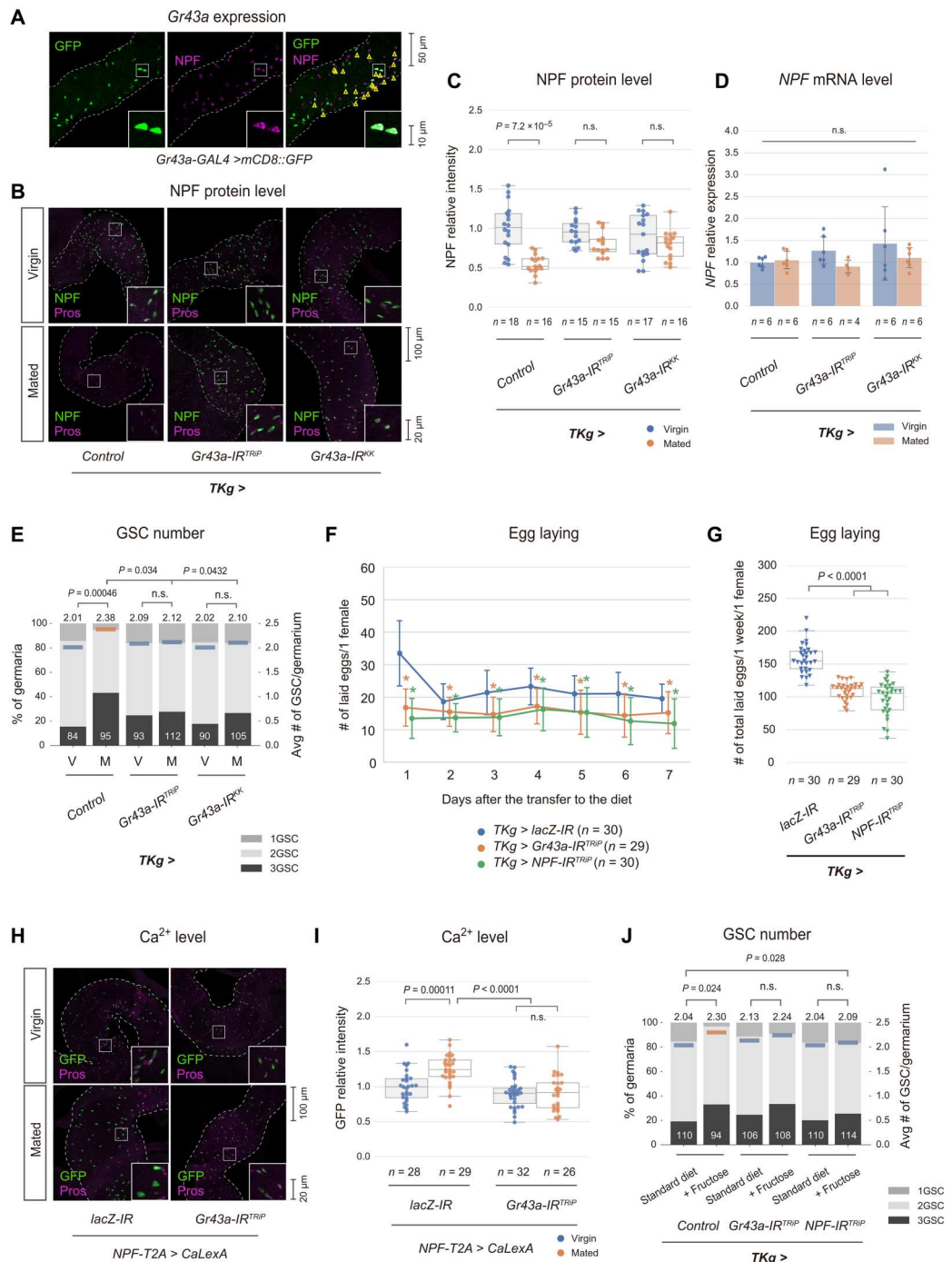
Notably, while basal levels of *NPF* mRNA in the gut were elevated in *R46G06-GAL4*-driven *Gr43a* RNAi and *Gr43a* genetic loss-of-function mutant females, compared to control virgin and mated females (fig. S5, C and F), such elevation was not observed in *Tkg-GAL4*-driven *Gr43a* RNAi females (Fig. 4D). Therefore, *NPF* expression in the gut seems to be influenced by Gr43a in peripheral sensory organs.

In terms of GSCs, *Tkg-GAL4*-driven RNAi animals are phenocopies of *R46G06-GAL4*-driven animals, as mating-induced increases in GSC numbers and pMad intensity in GSCs were also impaired by *Tkg-GAL4*-driven *Gr43a* RNAi (Fig. 4E and fig. S7, B and C). Consistent with their GSC proliferation phenotype, mated *Tkg-GAL4*-driven *Gr43a* RNAi female flies laid fewer eggs than mated control females (Fig. 4, F and G), which phenocopied *Tkg-GAL4*-driven *NPF* RNAi female flies, as previously reported (17). These data suggest that Gr43a in *NPF*⁺ EECs have a positive impact not only on GSC proliferation but also on reproductive fitness after mating.

It is thought that Gr43a is coupled with Ca²⁺ as a second messenger (29, 31). On the other hand, it has been reported that intracellular Ca²⁺ levels in EECs are elevated in response to dietary nutrients (32). Therefore, we examined whether loss-of-*Gr43a*-function EECs failed to elevate intracellular Ca²⁺ levels in EECs using the genetically encoded Ca²⁺ sensor, CaLexA (33). As expected, in control females, the fluorescence signal of the sensor in EECs was elevated in *NPF*⁺ EECs after mating (Fig. 4, H and I). In contrast, CaLexA signals in EEC-specific *Gr43a* knockdown flies were not elevated after mating. These results suggest that Gr43a is required for mating-induced Ca²⁺ elevation in EECs, which may be associated with mating-induced NPF release from EECs. We also found that there was no significant change in *Gr43a* expression in the midgut between virgin and mated females (fig. S5I), implying that the mating-induced NPF release is not simply due to the increased sensitivity to fructose in *NPF*⁺ EECs via Gr43a after mating.

Given that Gr43a is the taste receptor specific for fructose (29), we speculated that excessive fructose administration results in GSC increase even in virgin females. This is the case, as fructose administration on the standard diet leads to an increase in GSC numbers in control virgin females (Fig. 4J). The effect of excessive fructose on the GSC increase was not observed in *Tkg-GAL4*-driven *Gr43a*

Fig. 4. Gr43a in NPF-positive EECs is essential for the mating-induced enteroendocrine NPF release and GSC increase. (A) *Gr43-GAL4*-driven green fluorescent protein (GFP) signal (green) with anti-NPF immunostaining signal (magenta) in the middle midgut region of wild-type females. Scale bar, 50 μm . (B and C) NPF protein levels in *NPF*⁺ EECs of *Tkg-GAL4*-driven *Gr43a* and *lacZ* (control) RNAi animals. (B) Representative images of anti-NPF (green) and anti-Pros (pan-EEC marker; magenta) immunostaining in the middle midgut. (C) Quantification of anti-NPF signal intensity in *NPF*⁺ EECs. Box-and-whisker plots are also represented. (D) The abundance of *NPF* mRNA in the gut, as determined by RT-qPCR. (E) Frequencies of germaria containing one, two, and three GSCs and the average number of GSCs per gerarium in virgin and mated females of *Tkg-GAL4*-driven *Gr43a* RNAi and control animals. Data are represented as in Fig. 1C. (F) Temporal change in numbers of laid eggs. Values are presented as the mean with SD. Asterisks indicate $P < 0.05$ between *Gr43* RNAi and control females. For data acquisition, 30, 29, and 30 vials were prepared for *lacZ*, *Gr43a*, and *NPF* RNAi females, respectively. (G) Total numbers of laid eggs for 1 week. (H and I) Levels of CaLexA signals in *NPF-T2A-GAL4*-mediated *Gr43a* RNAi and control animals. (H) Representative images of immunofluorescent staining of CaLexA (green) and anti-Pros (magenta). Scale bar, 100 μm . (I) Quantification of CaLexA signals in *NPF*⁺ EECs. (J) Frequencies of germaria containing one, two, and three GSCs and the average number of GSCs per gerarium in females of *Tkg-GAL4*-driven *Gr43a* RNAi, *NPF* RNAi, and control animals that were fed standard diets supplemented with or without fructose. Data are represented as in (E). Statistical analysis: Wilcoxon rank sum test with Holm's correction for (C), (E), (I), and (J); and Tukey-Kramer's HSD for (D), (F), and (G). n.s., $P > 0.1$.



RNAi or *NPF* RNAi virgin females (Fig. 4J). These results suggest that fructose is essential for the NPF-mediated GSC increase via enteroendocrine *Gr43a* after mating.

Levels of hemolymph sugars, including fructose, are elevated after mating

Our nutritional analysis revealed that there was no detectable fructose in the glucose diet (Fig. 3A and table S1). Nevertheless, the glucose diet was sufficient to ensure a mating-induced GSC increase (Fig. 3C). The fact that the fructose receptor, *Gr43a*, is required for

mating-induced NPF release raises the possibility that glucose-derived metabolites, possibly fructose, are involved in the mating-induced GSC increase. Accordingly, we investigated metabolomic changes in wild-type flies reared on the standard diet before and after mating. Compared to the metabolic changes in whole bodies of virgin and mated females (Fig. 5, A and B, fig. S8A, and data S1), metabolites in hemolymph were drastically changed different between them (Fig. 5, C and D, fig. S8B, and data S1). Among 183 metabolites analyzed in this study, 43 hemolymph metabolites exhibited more than twofold changes ($P < 0.05$). Of those, erythrose

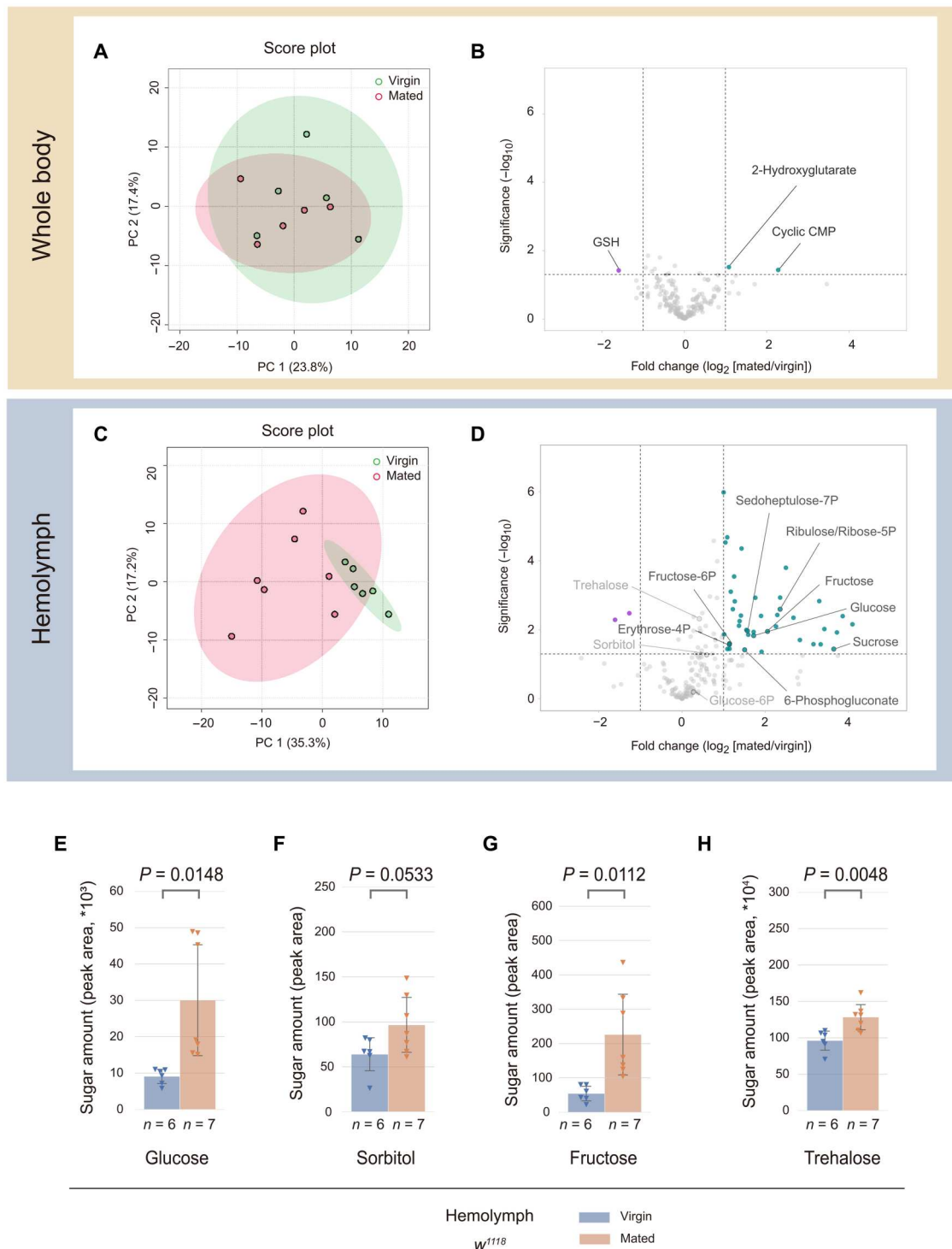


Fig. 5. Levels of hemolymph sugars, including fructose, are elevated after mating. (A to D) Metabolomic changes in samples derived from whole bodies (A and B) and hemolymph (C and D), based on raw data shown in data S1. Also, see fig. S8. (A and C) Principal components (PC) analysis plot of metabolome data. Ellipses of clusters show the 95% confidence regions for each sample group. Note that metabolomic profiles were clearly distinct between virgin and mated females in hemolymph but not whole-body samples. (B and D) Volcano plots to represent amounts of analyzed chemical compounds. The x axis represents the mean ratio fold change (\log_2 scale) of the relative abundance of each metabolite between virgin and mated females. Dashed lines on the x axis indicate 0.5- and 2-fold changes. The y axis represents P values ($-\log_{10}$ scale). The dashed line on the y axis indicates $P = 0.05$. Representative metabolites are described. CMP, cytidine monophosphate; GSH, glutathione (reduced form). (E to H) Levels of glucose (E), sorbitol (F), fructose (G), and trehalose (H) in hemolymph samples derived from wild-type virgin and mated females. Samples were analyzed with liquid chromatography–tandem mass spectrometry (LC-MS/MS) to measure glucose, fructose, and trehalose and with gas chromatography–mass spectrometry (GC-MS) to measure sorbitol. The amount of each sugar is represented as a peak area of mass spectrometric metabolome analysis. Statistics: Welch's t test.

4-phosphate, fructose 6-phosphate, 6-phosphogluconate, ribose/ribose 5-phosphate, and sedoheptulose 7-phosphate, all of which are produced via the pentose phosphate pathway, were elevated in mated females, compared to virgin females (Fig. 5D). This observation is consistent with a previous report showing the importance of the pentose phosphate pathway for egg production in *Drosophila* (15). Other hemolymph metabolites elevated after mating were sugars, including glucose, sorbitol, trehalose, and fructose (Fig. 5, E to H). These results support our hypothesis that hemolymph fructose is essential for regulating mating-induced NPF secretion and GSC increase.

The polyol pathway is essential for NPF release from EECs after mating

In eukaryotes, fructose is synthesized from glucose via the polyol pathway, in which glucose is first converted to sorbitol, followed by conversion to fructose (34). One of the critical enzymes for the polyol pathway is sorbitol dehydrogenase (Sodh), responsible for conversion of sorbitol to fructose (Fig. 6A). Therefore, we wondered whether Sodhs is required for mating-induced NPF secretion and GSC increase. Because the *D. melanogaster* genome has two *Sodh* genes, *Sodh-1* and *Sodh-2*, we used a double loss-of-function genetic mutant of *Sodh-1* and *Sodh-2* that was previously generated (35). Hereafter, we designate the double mutant strain as the "Sodh mutant."

We first examined levels of hemolymph sugars in *Sodh* mutant virgin and mated females. In both, hemolymph sorbitol was drastically up-regulated in mated females, compared to virgin females (Fig. 6B). This observation fits the biochemical function of Sodhs, as sorbitol, the enzyme substrate, should accumulate if Sodh is eliminated. We found that mating-induced elevation of hemolymph fructose was suppressed in *Sodh* mutant females (Fig. 6C). It was unlikely that the phenotypes were due to failure of mating, as almost all females of both control (*Sodh* heterozygotes) and *Sodh* mutant were mated (fig. S9A). These results suggest that the polyol pathway is required for elevation of hemolymph fructose after mating.

We next examined NPF protein levels in virgin and mated female *Sodh* mutants. When *Sodh* mutant females were reared on the standard diet, NPF protein levels in EECs were not reduced after mating (Fig. 6, D and E). When *Sodh* mutant flies reared on the standard diet were transferred into a modified standard diet supplemented with sorbitol or fructose, impairment of the NPF reduction in EECs after mating was restored on the fructose-supplemented diet, but not that supplemented with sorbitol (Fig. 6, D and E), consistent with conversion by the polyol pathway. In *Sodh* mutants reared on fructose- or the sorbitol-supplemented standard diet, *NPF* mRNA levels were not changed before or after mating, whereas levels were increased, compared to the standard diet without sugar supplements (Fig. 6F). Instead of the fructose-supplemented standard diet, we also took a similar experimental approach using a modified standard diet in which glucose was replaced with fructose. We observed the same phenotypes in regard to levels of NPF protein and *NPF* mRNA in *Sodh* mutant guts (fig. S9, B to D). These results suggest that elevation of fructose, mediated by the polyol pathway, is essential for NPF release from EECs after mating.

A previous study revealed that *Sodh* mutant larvae exhibit reduced levels of triacylglyceride (TAG) in fat bodies (35). In

addition, enteroendocrine NPF regulates the TAG level in adult fat bodies systemically in insulin-like peptide- and adipokinetic hormone-dependent manners (20). Moreover, metabolic pathways in fat bodies control the female GSC lineage (16). These studies raise the possibility that mating-induced NPF release from EECs may affect TAG levels in mated females. However, while the TAG level of *TKg-GAL4*-driven *NPF* RNAi virgin females decreased compared to control virgins, consistent with our previous study (20), there was no significant difference in TAG levels between control and *TKg-GAL4*-driven *NPF* RNAi mated females (fig. S10). These results suggest that TAG levels are not regulated by the mating-fructose-Gr43a-NPF axis and imply that the axis makes little or no contribution to regulation of TAG levels in mated females.

Fructose generated by the polyol pathway is required for the mating-induced, NPF-mediated GSC increase

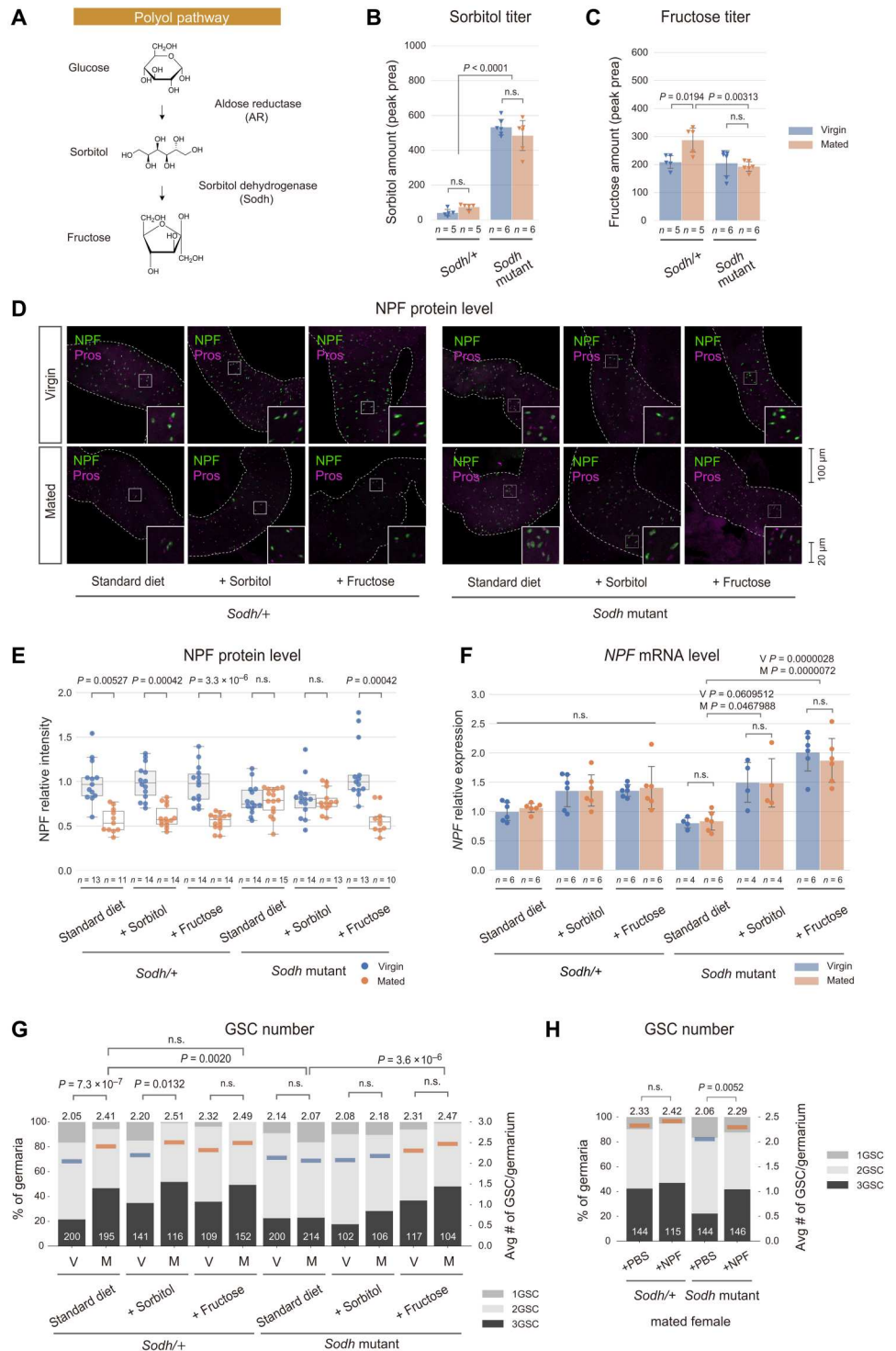
Consistent with enteroendocrine NPF levels, the mating-induced GSC increase was impaired in *Sodh* mutant females reared on the standard diet (Fig. 6G). Consistent with the decrease in GSC numbers, laid, fertilized eggs of *Sodh* mutant females on the standard diet were fewer than those of control females (fig. S9, E and F). In contrast, GSC numbers after mating were increased in *Sodh* mutants on the standard diet supplemented with fructose, but not with sorbitol (Fig. 6G), or the modified standard diet in which glucose was replaced with fructose (fig. S9G). It was unlikely that these phenotypes are a secondary effect of malnutrition, as there were no differences in food consumption between control and *Gr43a* genetic loss-of-function mutants (fig. S9H). We found that injection of synthetic NPF peptides into *Sodh* mutant females resulted in increased GSC numbers, compared with injections of PBS vehicle, regardless of mated or unmated status (Fig. 6H). These results suggest that circulating NPF is crucial for the fructose-mediated GSC increase.

Besides Sodhs, aldose reductases (ARs) are also critical for the polyol pathway (Fig. 6A). Therefore, we conducted phenotypic analyses on a double loss-of-function mutant of two putative *AR* genes, *CG6084* and *CG10638* (35), which are designated *AR* mutants, hereafter. We found that neither NPF protein levels in EECs nor *NPF* mRNA levels were changed in virgin or mated *AR* mutant females (fig. S11, A to C). In addition, the mating-induced GSC increase was also impaired in *AR* mutant females (fig. S11D), suggesting that loss of function of ARs also phenocopied *Sodh* mutant females.

We next examined whether polyol pathway-related genes were changed transcriptionally after mating. At the whole-body level, no genes were significantly higher in mated females than in virgin females (fig. S12A). Rather, *Sodh1* expression showed a decreasing trend. We also examined expression levels of genes in the carcass containing muscles, epidermis, and fat bodies (fig. S12B), and the guts (fig. S12C), as a recent large-scale transcriptomic analysis revealed that most *Sodh* and *AR* genes are highly expressed in these tissues (36). Except for the decrease in *Sodh1* expression in the carcass and guts and the increase in *mlx* expression in the carcass, no other genes were differentially expressed before or after mating in either the carcass or the guts. Therefore, we conclude that mating-induced fructoseogenesis cannot be explained by transcriptional regulation of the polyol pathway. Together, these results suggest that mating-induced fructoseogenesis by the polyol

Fig. 6. *Sodh* is required for fructoseogenesis after mating.

(A) Schematic representation of the polyol pathway. Aldose reductase (AR) and *Sodh* are responsible for the conversion of glucose to sorbitol and to sorbitol and fructose, respectively. **(B and C)** Amounts of sorbitol (B) and fructose (C) in hemolymphs of control (*Sodh*^{+/+}) and *Sodh* homozygous mutant females. Samples were analyzed with GC-MS to measure sorbitol and with LC-MS/MS to measure fructose. Amounts of each sugar are represented as a peak area in the mass spectrometric metabolome analysis. **(D to F)** Levels of NPF protein and *NPF* mRNA in the middle midgut of control (*Sodh*^{+/+}) and *Sodh* homozygous mutant females reared on the standard diet without any supplements, with sorbitol (+sorbitol), and with fructose (+fructose) for 3 days (D) Representative images of anti-NPF (green) and anti-Pros (pan-EEC marker; magenta) immunostaining in *NPF*⁺ EECs. (E) Quantification of anti-NPF signal intensity in *NPF*⁺ EECs. Box-and-whisker plots are also presented. (F) Abundance of *NPF* mRNA in the guts, as determined by RT-qPCR. **(G and H)** Frequencies of germaria containing one, two, and three GSCs (left vertical axis) and the average number of GSCs per germarium (orange and blue horizontal lines, corresponding to the right vertical axis), respectively. Numbers in bars indicate numbers of germaria that we observed. Germaria for each experimental condition were derived from 10 to 20 females. (G) Control (*Sodh*^{+/+}) and *Sodh* homozygous mutant females reared on the standard diet without any supplements, with sorbitol (+sorbitol), and with fructose (+fructose). (H) Mated females of control (*Sodh*^{+/+}) and *Sodh* homozygous mutant, injected with PBS (control) and synthetic NPF peptides. Statistical analysis: Tukey-Kramer's HSD test for (B), (C), and (F); and Wilcoxon rank sum test with Holm's correction for (E), (G), and (H). n.s., *P* > 0.1.



pathway serves an essential function in the mating-induced GSC increase via regulation of NPF release from EECs.

Fructose does not directly act on the ovary to regulate the GSC increase

A previous study reported that sugar metabolism is drastically changed in the ovary after mating (15). We realized that

hemolymph levels of glucose, fructose, and trehalose did not increase significantly after mating in *Tkg-GAL4*-driven *Gr43a* RNAi animals (fig. S13), suggesting that midgut *Gr43a* affects systemic sugar metabolism via enteroendocrine NPF. These data raise the possibility that not only circulating NPF but also hemolymph sugars, including fructose itself, may directly stimulate the ovary to induce the mating-induced GSC increase. To test this possibility,

we conducted *ex vivo* ovary culture experiments to examine tissue culture media supplemented with fructose, glucose, or trehalose (fig. S14A). Using this system, we previously demonstrated that supplementation of synthetic NPF peptide is sufficient to induce the GSC increase in ovaries dissected from virgin females (17). However, we found no effects of these sugars on the GSC increase in the same *ex vivo* experimental system (fig. S14, B to D). Therefore, it is unlikely that fructose and other sugars directly act on the ovary to regulate the GSC increase. Together, all results in this study suggest that hemolymph fructose regulates release of enteroendocrine NPF, leading to a dietary sugar-dependent, mating-induced GSC increase (Fig. 7).

DISCUSSION

In general, dietary sugars, particularly glucose, directly affect metabolic status in almost all cells of living organisms, including cells of the germline lineage in *D. melanogaster* (15). However, it is unlikely that dietary glucose directly acts on GSCs or other ovarian cells to regulate the mating-induced GSC increase. Rather, dietary glucose contributes to elevation of hemolymph fructose generated by a metabolic pathway called the polyol pathway. Elevated fructose is required for a mating-induced release of enteroendocrine NPF from the midgut via the fructose-specific Gr, Gr43a, followed by an NPF-mediated increase in GSCs after mating. This study illustrates that dietary sugars are indispensable prerequisites for the GSC increase after mating, leading to an enhancement of egg production. Our results also demonstrate that not only proteins but also sugars are essential dietary nutrients that influence GSCs.

One of the important findings of this study is that circulating fructose, derived from dietary glucose, acts as a signal to regulate enteroendocrine hormone release after mating. While the most common dietary sugars, including glucose, trehalose, and fructose, are all circulating in hemolymph and are used as an important energy source in cells, fructose serves some unique functions. First, the circulating fructose level is 100 times less than circulating levels of glucose and trehalose, the major circulating sugars, in both fruit flies and mammals, although substantial amounts of fructose

are contained in a wide variety of foods, including fruits. Second, in contrast to the fact that glucose and trehalose in hemolymph increase several times after feeding, fructose can rise >50-fold after a sugary meal in mammals (37) and 3- to 10-fold after carbohydrate diets in adult *D. melanogaster* (29). Third, studies on *D. melanogaster* have demonstrated that circulating fructose mediates neuronal activity in the brain and regulates satiety-dependent feeding behavior (29, 38). Therefore, we speculate that low and high circulating fructose reflect hunger and satiety, respectively, leading to nutrient-dependent physiological regulation in organismal tissues, including the brain (29, 38), fat bodies (35), and EECs (this study). On the other hand, in *Sodh* mutant animals, the mating-induced NPF release and GSC increase did not occur although hemolymph fructose was not elevated after mating but still present at substantial levels (Fig. 6, C to E and G). These results imply that there must be a critical threshold of hemolymph fructose to drive mating-induced events, although the mechanism by which such a threshold is established has not been determined.

This study also reveals the physiological role of the polyol pathway in the context of a postmating response. The polyol pathway has long been known as the metabolic reaction that converts glucose to fructose. In addition, previous studies have suggested that overactivation of the polyol pathway affects diabetes-induced oxidative stress (39). However, it is still unclear whether and how the polyol pathway contributes to normal physiological phenomena. Very recently, it was reported that the polyol pathway contributes to metabolic reprogramming through regulation of Mondo/ChREBP-dependent gene expression (35). In this study, we reveal another role of the polyol pathway in the mating-dependent GSC increase and egg production. We propose that hemolymph fructose, generated by the polyol pathway, serves as an indispensable signal to ensure that females accumulate enough dietary energy to support oogenesis. Therefore, this study expands our understanding of the importance of the polyol pathway. To further understand the relationship between mating and the polyol pathway, an important remaining question is how mating regulates activity of the polyol pathway. Genes related to the polyol pathway are not up-regulated at transcriptional levels, implying that the polyol pathway seems to be activated at the posttranscriptional or enzymatic level by unknown mechanisms.

It is noteworthy that phenotypes of *AR* and *Sodh* mutants are almost fully rescued by oral administration of fructose. Under our experimental conditions, we used 10% fructose in foods, which is nearly equal to the amount of fructose (including the derivative from sucrose) in some fruits that *D. melanogaster* consumes in the wild, such as apples and grapes (40). This situation paradoxically raises the possibility that the polyol pathway may not be necessary for the mating-induced NPF release from EECs and the subsequent GSC increase in the wild. However, we note that many other natural food sources for *D. melanogaster*, such as tomatoes (41), contain only 1 to 2% fructose (40). Therefore, we speculate that the polyol pathway may be indispensable even in the wild, as fructose must be generated to reflect systemic hunger/satiety status, even when the flies are fed low-fructose diets. On the other hand, there may be polymorphisms that affect the polyol pathway depending on the type of fruits available in different geographic areas. Therefore, ecological aspects of the polyol pathway would be intriguing to study in the future.

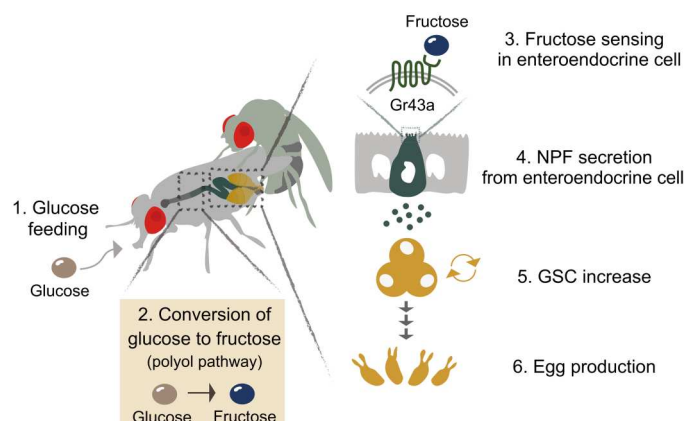


Fig. 7. Graphical summary of this study. Dietary glucose contributes to the elevation of hemolymph fructose after mating, which is generated by the polyol pathway. Elevated fructose stimulates Gr43a in *NPF*⁺ EECs, leading to NPF secretion. Secreted NPF is received by ovarian somatic cells and enhances the GSC increase and mature egg production.

Another noteworthy finding of this study was that fructose-mediated control of NPF release from EECs depends on the fructose taste receptor, Gr43a. Gr43a is one of nine identified sugar-sensing receptors present in peripheral Gr neurons in taste organs, such as the proboscis and legs (26, 29). Beside peripheral neuronal expression, a pioneering study by Miyamoto *et al.* (29) found that *Gr43a* is expressed in the brain. Moreover, they found that brain Gr43a is both necessary and sufficient to sense circulating fructose and to promote feeding in hungry flies but suppresses feeding in satiated flies. A recent study also revealed that *Gr43a*-expressing central neurons are part of the neuronal circuit necessary for precise satiety-dependent control of feeding behavior (38). On the other hand, because previous studies have revealed that *Gr43a* is expressed in other cell types, including midgut EECs (24), additional roles of internal fructose-sensing mechanisms via Gr43a have been discussed (29). This study confirms that this is the case.

Various types of evidence in this study imply that Gr43a in EECs may sense fructose in hemolymph, but not in the gut lumen, as a diet without fructose still contributes to the mating-induced NPF release through elevation of circulating fructose generated by the polyol pathway. However, the subcellular distribution of Gr43a in EECs has not been investigated. Because dietary fructose also affects NPF release from EECs, the possibility that Gr43a also senses fructose in the gut lumen cannot be excluded. It must also be noted that *Gr43a* is only expressed in ~70% *NPF*⁺ EECs. In contrast, mating-induced NPF release was observed in almost all *NPF*⁺ EECs. These findings imply that the Gr43a-independent mechanism may be involved in mating-induced NPF release. On the basis of results of our RNAi experiments, *Gr5a*, *Gr64a*, and *Gr64f*, encoding sugar taste receptors that sense trehalose specifically and many types of sugars, respectively, are candidates to contribute to the mating-induced NPF release, while their expression in *NPF*⁺ EECs was not confirmed. Alternatively, sugar transporters may contribute to NPF release from EECs, because fructose induces glucagon-like peptide-1 (GLP-1) secretion through the fructose transporter, GLUT5, in mammals (42, 43). However, RNAi of the previously reported sugar transporter, *Sut1*, which is required for dietary sugar-stimulated NPF release in virgin females (20), did not affect NPF release in mated females. A very recent study also reported that *Sut1* in EECs is not involved in enteroendocrine NPF-dependent regulation of protein-rich food preference in *D. melanogaster* (44). Curiously, this study revealed that *Sut2*, another type of SLC2 sugar transporter, is involved in NPF production or release in midgut EECs to regulate protein-rich food preference in mated females (44). Therefore, it would be intriguing to examine whether *Sut2* in EECs is involved in the mating-induced GSC increase. Moreover, in future studies, a recently developed single-cell RNA sequencing database of EECs (30) might be helpful for identifying additional factors that regulate mating-induced NPF release from *NPF*⁺ EECs.

A question to be addressed in future studies is whether the indispensable role of circulating fructose in reproduction also exists in mammals. In humans and other mammals, high sugar levels are developed during pregnancy, known as gestational diabetes. It is thought that human gestational diabetes is caused by insulin resistance due to elevation of several hormones during pregnancy, including human placental lactogen, estrogen, and progesterone (45–47). It is intriguing to examine whether high blood glucose leads to elevation of blood fructose generated by the polyol

pathway during pregnancy. Regarding the effect on EECs, it has already been reported that fructose stimulates GLP-1 but not GIP secretion in mice, rats, and humans (42). GLP-1 secretion from EECs is regulated, at least in part, by the heteromeric taste receptor consisting of Taste Receptor type 1 members 2 and 3 (T1R2/T1R3), which provoke release of GLP-1 and GIP (48, 49). Moreover, T1R2/T1R3 can sense fructose (50). Therefore, although Gr43a is not conserved in vertebrates, fructose may influence secretion of GLP-1, which is a functional counterpart of *D. melanogaster* enteroendocrine NPF (20), through mammalian taste receptors that sense fructose in EECs. Further clarification of the role of fructose and its taste receptor in mammals should be fascinating. This clarification will be valuable to understand the deleterious effects of fructose, as excessive dietary fructose consumption of mothers entails a postnatal risk of diseases in their offspring (51, 52).

MATERIALS AND METHODS

D. melanogaster strains and husbandry

Fly stocks were maintained on a standard diet (0.55 g of agar, 10.0 g of glucose, 9.0 g of cornmeal, 4.0 g of yeast extract, 300 μ l of propionic acid, 350 μ l of 10% butylparaben in 70% ethanol, and 100 ml of water). All experiments were conducted at 25°C under a 12:12-hour light/dark cycle.

The following strains were obtained from the Bloomington *Drosophila* Stock Center (BDSC): *dj-GFP* (18) (no. 5417), *NPF-T2A-GAL4* (53) (no. 84671), *R46G06-GAL4* (54) (no. 41271), *UAS-mCD8::GFP* (no. 32186), *UAS-lacZ* (no. 8529), and *UAS-CaLexA* (33) (no. 66542). The following transgenic RNAi project (TriP) lines were also obtained from BDSC: *UAS-NPF-IR^{TRiP}* (no. 27237), *UAS-Gr5a-IR^{TRiP}* (no. 31282), *UAS-Gr36c-IR^{TRiP}* (no. 64901), *UAS-Gr43a-IR^{TRiP}* (no. 64881), *UAS-Gr64b,Gr64c-IR^{TRiP}* (no. 36734), *UAS-Gr64d,Gr64e-IR^{TRiP}* (no. 37497), and *UAS-Gr64f-IR^{TRiP}* (no. 65034). The following transgenic RNAi strains were obtained from the Vienna *Drosophila* Resource Center: *UAS-Sut1-IR^{KK}* (no. 104983), *UAS-Gr28b-IR^{SH}* (no. 330295), *UAS-Gr33a-IR^{KK}* (no. 101615), *UAS-Gr43a-IR^{KK}* (no. 107681), *UAS-Gr61a-IR^{KK}* (no. 106007), *UAS-Gr64a-IR^{KK}* (no. 103342), and *UAS-Gr93a-IR^{KK}* (no. 105595). Note that *Gr43a-IR^{TRiP}* and *Gr43a-IR^{KK}* express two independent transgenic RNAi hairpin constructs (Fig. 4, B to E).

Other strains used in this study were as follows: the *Sodh* mutant (double mutant of *Sodh1* and *Sodh2*) (35), the *AR* mutant (double mutant of *CG6084* and *CG10638*) (35), *Tkg-GAL4* (21), and *UAS-lacZ-IR* (55) (gifts from M. Miura, the University of Tokyo, Japan); the *Gr43a* mutant, in which a *GAL4* construct is inserted in the *Gr43a* locus (29) (a gift from C. Miyamoto and H. Amrein, Texas A&M University, USA); and *Gr5a-GAL4* (56), *Gr43a-GAL4* (56), and *Gr64f-GAL4* (56) (gifts from J. R. Carlson, Yale University, USA). *UAS-NPF* was established in this study, as described later.

w¹¹¹⁸ was used as the wild type. All data were obtained from females in this study. For the experiments represented in Fig. 4D [quantitative reverse transcription polymerase chain reaction (RT-qPCR)], Fig. 4F (egg-laying assays), Fig. 4G (egg-laying assays), Fig. 4I (CaLexA experiments), fig. S7A (copulation assays), fig. S10 (TAG measurements), and fig. S13 (hemolymph sugar level measurements), *lacZ* RNAi (with *UAS-lacZ-IR* strain) was used as a control. For the NPF overexpression experiment (fig. S2C), *lacZ* overexpressor (with *UAS-lacZ* strain) was used as a control. For

all other experiments, heterozygous controls were obtained by crossing w^{1118} to strains of genetic mutants, GAL4 drivers, and UAS effectors.

Establishment of *UAS-NPF* transgenic flies

For generation of the *UAS-NPF* plasmid, the coding sequence of *NPF* was amplified by PCR with adult w^{1118} gut complementary DNA (cDNA) using the primers UAS-NPF_F1EcoRI and UAS-NPF_R1XbaI (table S2). PCR products were digested with Eco RI and Xba I and subsequently cloned into the Eco RI–Xba I–digested pWALIU10-moe vector (57). The *NPF*-pWALIU10-moe (*UAS-NPF* plasmid) was then injected into $y^1 w^+$ $P\{y^{+17.7}=nanos-phiC31\int int.NLS\}X$; $P\{y^{+17.7}=CaryP\}attP40$ embryos by WellGenetics Inc.

Feeding assay and food contents

Adult flies were raised for 5 days at 25°C on the standard diet and then reared for additional days, depending on each experiment, on diets containing different nutrients. Recipes for making different diets are described in table S1. Proportions of raw materials in each of the diets (weight/water volume) are as follows (also see Fig. 1A):

Standard diet: 0.55% agar, 4% dry yeast, 10% glucose, and 9% cornmeal.

Yeast diet (Figs. 1, A and C to F; 2, A to F; and 3, C to E; and figs. S1B and S2, A and B): 0.55% agar and 4% dry yeast.

Cornmeal diet (Figs. 1, A and C, and 3A): 0.55% agar and 9% cornmeal.

YC diet (Figs. 1, A and C, and 3A): 0.55% agar, 4% dry yeast, and 9% cornmeal.

Glucose diet (Figs. 1, A and C, and 3, A and C to E): 0.55% agar and 10% glucose.

YG diet (Figs. 1, A and C, and 3A): 0.55% agar, 4% dry yeast, and 10% glucose.

Sucrose diet (Fig. 3, C to E): 0.55% agar, 4% dry yeast, and 10% sucrose.

The modified standard diet supplemented with fructose (Figs. 4J and 6, D to G): 0.55% agar, 4% dry yeast, 10% glucose, 9% cornmeal, and 10% fructose.

The modified standard diet supplemented with sorbitol (Fig. 6, D to G): 0.55% agar, 4% dry yeast, 10% glucose, 9% cornmeal, and 10% sorbitol.

The modified standard diet in which glucose was replaced with fructose (fig. S9, B to D and G): 0.55% agar, 4% dry yeast, 9% cornmeal, and 10% fructose.

Antibody preparation

An antibody against NPF protein was raised in rabbits. A keyhole limpet hemocyanin–conjugated synthetic peptide used for immunization was previously described (20).

Immunohistochemistry and microscopic observation

Ovaries and midguts were dissected in Schneider's *Drosophila* medium (Thermo Fisher Scientific 21720024) and fixed in 4% paraformaldehyde in PBS for 30 to 60 min at room temperature. Fixed samples were washed three times in PBS. For immunostaining with gut samples, washed samples were rinsed stepwise with 30, 50, and 70% ethanol, followed by a 10-min incubation with 90% ethanol. Samples were blocked in a blocking solution (PBS with 0.1%

Triton X-100 and 0.2% bovine serum albumin) for 1 hour at room temperature and then incubated with a primary antibody in blocking solution at 4°C overnight. Primary antibodies used in this study were mouse anti-Hts 1B1 [Developmental Studies Hybridoma Bank (DSHB); 1:50], rat anti-E-cadherin DCAD2 (DSHB; 1:50), mouse anti-Prospero antibody MR1A (DSHB; 1:50), rabbit monoclonal anti-pMad (Abcam ab52903; 1:1000), mouse anti-Lamin-C LC28.26 (DSHB; 1:10), rabbit anti-NPF (this study; 1:2000), and chicken anti-green fluorescent protein (GFP; Abcam ab13970; 1:8000). When anti-pMad, anti-Hts 1B1, or anti-E-cadherin DCAD2 antibody was used, immunofluorescent signals were enhanced by Can Get Signal Solution B (ToYoBo). After washing, fluorophore (Alexa Fluor 488 or 546)–conjugated secondary antibodies (Thermo Fisher Scientific) were used at a 1:200 dilution, and samples were incubated for 2 to 3 hours at room temperature in blocking solution. After another washing step, all samples were mounted in FluorSave reagent (Merck Millipore).

Samples were visualized using a Zeiss LSM 700 confocal microscope or a Zeiss Axioplan 2. Fluorescence intensity in confocal sections was measured using ImageJ software. GSC numbers were determined on the basis of morphology and positioning of their anteriorly anchored spherical spectrosomes (58). For GSC number quantification, germaria for each experimental condition were derived from 10 to 20 females. For NPF quantification, an average of five cells was examined for each midgut. For pMad quantification, signal intensity was calculated by measuring fluorescence intensity in GSCs.

Quantitative reverse transcription PCR

To quantify *NPF* mRNA levels, midguts of 8 to 10 adult female flies (5 to 6 days after eclosion) were dissected for each sample. Total RNA was extracted using RNAiso Plus reagent (TaKaRa). cDNA was prepared with ReverTra Ace qPCR RT Master Mix with gDNA Remover (TOYOBO). RT-qPCR was performed using THUNDERBIRD NEXT SYBR qPCR Mix (TOYOBO) with a Thermal Cycler Dice TP800 system (TaKaRa). Serial dilutions of a plasmid containing the open reading frame of each gene were used as standards. The amount of target mRNA was normalized to *ribosomal protein 49* (*rp49*) and then relative fold changes were calculated. Primers used in this study are described in table S2. The primers for *rp49* and *NPF* were previously described (20).

Fly injection

Injections of the synthetic NPF peptide into virgin females were performed as previously described (17). In this study, GSC numbers and pMad intensity were examined 12 hours after NPF injection.

Hemolymph collection

For hemolymph extractions, 40 female flies were perforated with a tungsten needle and placed in a 0.5-ml plastic tube perforated with a 27-G needle. These tubes were placed inside 1.5-ml plastic tubes and centrifuged for 5 min at 5000g at 4°C to collect hemolymph, followed by collection of a 1 μ l of hemolymph aliquot from each tube.

Measurement of whole-body and hemolymph metabolites by liquid chromatography–tandem mass spectrometry and gas chromatography–mass spectrometry

A widely targeted metabolomics analysis was done as described previously (59, 60). In brief, each frozen sample in a 1.5-ml plastic tube was homogenized in 300 μ l of cold methanol with a single ϕ 3-mm zirconia bead using a microtube homogenizer (TAITEC Corp.) at 41.6 Hz for 2 min. Homogenates were mixed with 200 μ l of methanol, 200 μ l of H₂O, and 200 μ l of CHCl₃ and vortexed for 20 min at room temperature. Samples were centrifuged at 20,000g for 15 min at 4°C. The insoluble pellets were used to quantify total protein using a BCA protein assay kit (Thermo Fisher Scientific). Supernatant was mixed with 350 μ l of H₂O, vortexed for 10 min at room temperature, and centrifuged at 20,000g for 15 min at 4°C. The aqueous phase was collected, divided into two tubes, and dried in a vacuum concentrator.

For liquid chromatography–tandem mass spectrometry (LC-MS/MS) analysis, samples were redissolved in 2 mM ammonium bicarbonate (pH 8.0). Chromatographic separations in an Acquity UPLC H-Class System (Waters) were carried out under reverse-phase conditions using an ACQUITY UPLC HSS T3 column (100 mm by 2.1 mm, 1.8- μ m particles, Waters) and under HILIC conditions using an ACQUITY UPLC BEH Amide column (100 mm by 2.1 mm, 1.8- μ m particles, Waters). Ionized compounds were detected using a Xevo TQD triple quadrupole mass spectrometer coupled to an electrospray ionization source (Waters). The peak area of target metabolites was analyzed using MassLynx 4.1 software (Waters).

For gas chromatography–mass spectrometry analysis, samples were redissolved in methoxyamine pyridine solution and oximated for 90 min at 30°C. Then, MSTFA + 1% TMCS (Thermo Fisher Scientific) was added and incubated for 60 min at 37°C for trimethylsilylation. Derivatized metabolites were analyzed with an Agilent 7890B GC coupled to a 5977A Mass Selective Detector (Agilent Technologies) using DB-5MS + DG column (30 m \times 0.25 mm, 0.25- μ m film thickness; Agilent Technologies). Metabolites were detected in selected ion monitoring (SIM) mode, and peak areas of interest were analyzed with QuantAnalysis software (Agilent Technologies). Metabolite signals in whole-body samples were normalized to the total protein level of the corresponding sample. Metabolite signals in hemolymph were expressed per microliter of sample. *P* values were calculated using the unpaired, two-tailed Welch's *t* test in Microsoft Excel. Further statistical analysis, including principal components analysis, was performed in MetaboAnalyst 5.0 (61). Data were normalized to the median per sample.

Measurement of sugar levels in fly diets by LC-MS/MS

Each raw material (dry yeast, cornmeal, glucose, or agar) was prepared at a concentration of 1 mg/ml in water and incubated at 95°C for 2 hours. To obtain hydrolysates, each raw material was incubated with amyloglucosidase (Sigma-Aldrich, 10102857001) at 37°C for overnight, and then samples were diluted in 10 volumes of acetonitrile and centrifuged at 20,000g for 15 min at 4°C. Supernatants were analyzed with LC-MS/MS to measure glucose and fructose. Glucose in the hydrolysates and fructose in raw materials were measured as described previously (62). Sample concentrations were calculated from the standard curve obtained from a serial dilution of the standard solution.

Triglyceride measurement

Measurement of whole-body triglycerides was conducted using a Serum Triglyceride Determination kit (Sigma-Aldrich, TR0100) as previously described (20).

Egg-laying assays

Flies were reared at 25°C and aged for 5 days on the standard diet. One virgin female was mated overnight to three *w*¹¹¹⁸ males at 25°C in a vial. Individual female flies were transferred to a fresh chamber with the standard diet, after which eggs were counted manually.

Capillary feeder assay

Measurement of food intake amounts by capillary feeder assay was conducted as previously described (20, 63).

Ex vivo ovary culture

Ex vivo ovary culture experiments were performed as described (17, 19). Adult females were cultured on the standard diet and dissected in Schneider's *Drosophila* medium. Approximately six ovaries were transferred to 35-mm plastic dishes containing 3 ml of Schneider's *Drosophila* medium supplemented with 10% fetal bovine serum and Penicillin-Streptomycin Solution (Fujifilm-Wako 168-23191; 1:100 dilution) with addition of fructose, glucose, or trehalose. Cultures were incubated at room temperature for 12 hours, and then samples were immunostained to count GSC numbers.

To determine the concentration of glucose to be added to the medium, we first measured hemolymph glucose concentrations of mated wild-type (*w*¹¹¹⁸) females as a reference. Measurements using Glucose Oxidase Assay Kits (Sigma-Aldrich GAGO-20) were conducted as described previously (20, 64). We found that postmating females had a hemolymph glucose concentration of 17.2 \pm 1.1 mg (six hemolymph samples, each of which was derived from 40 flies). Therefore, we conducted ex vivo ovary culture experiments by adding glucose to the culture medium at concentrations close to, less than, and greater than these concentrations (22, 2, and 82 mg/ml, respectively; fig. S14C). On the other hand, on the basis of the peak area data from LC-MS analysis (Fig. 5, E and G), the amount of hemolymph fructose was 10-fold less than that of hemolymph glucose. Therefore, we decided to apply a smaller dose of fructose than we did of glucose, namely, 0, 3, and 10 mg/ml of fructose (fig. S14B). As a previous study reported that the hemolymph trehalose concentration is about 20 mg/ml (64), we added trehalose at concentrations less and greater than these concentrations (2, 42, and 82 mg/ml, respectively; fig. S14D).

Statistical analysis

All experiments were performed independently at least twice. Sample sizes were chosen on the basis of the number of independent experiments required for statistical significance and technical feasibility. Experiments were not randomized, and investigators were not blinded. All statistical analyses were carried out in the "R" software environment. All data used for the statistical analysis are available in data S1, S2, and S3.

Supplementary Materials

This PDF file includes:

Figs. S1 to S14

Tables S1 and S2

Legends for data S1 to S3

Other Supplementary Material for this manuscript includes the following:

Data S1 to S3

[View/request a protocol for this paper from Bio-protocol.](#)

REFERENCES AND NOTES

1. A. R. Armstrong, *Drosophila melanogaster* as a model for nutrient regulation of ovarian function. *Reproduction* **159**, R69–R82 (2020).
2. V. Smykal, A. S. Raikhel, Nutritional control of insect reproduction. *Curr. Opin. Insect Sci.* **11**, 31–38 (2015).
3. M. F. Wolfner, M. Federica, S. H. Weiss, Battle and ballet: Molecular interactions between the sexes in *Drosophila*. *J. Hered.* **100**, 399–410 (2009).
4. K.-Y. Lin, H.-J. Hsu, Regulation of adult female germline stem cells by nutrient-responsive signaling. *Curr. Opin. Insect Sci.* **37**, 16–22 (2020).
5. T. Ameku, R. Niwa, Mating-induced increase in germline stem cells via the neuroendocrine system in female *Drosophila*. *PLOS Genet.* **12**, e1006123 (2016).
6. R. Hoshino, R. Niwa, Regulation of mating-induced increase in female germline stem cells in the fruit fly *Drosophila melanogaster*. *Front. Physiol.* **12**, 785435 (2021).
7. G. B. Carvalho, P. Kapahi, D. J. Anderson, S. Benzer, Allochre modulation of feeding behavior by the sex peptide of *Drosophila*. *Curr. Biol.* **16**, 692–696 (2006).
8. P. M. Itskov, J.-M. Moreira, E. Vinnik, G. Lopes, S. Safarik, M. H. Dickinson, C. Ribeiro, Automated monitoring and quantitative analysis of feeding behaviour in *Drosophila*. *Nat. Commun.* **5**, 4560 (2014).
9. R. Leitão-Gonçalves, Z. Carvalho-Santos, A. P. Francisco, G. T. Fioreze, M. Anjos, C. Baltazar, A. P. Elias, P. M. Itskov, M. D. W. Piper, C. Ribeiro, Commensal bacteria and essential amino acids control food choice behavior and reproduction. *PLOS Biol.* **15**, e2000862 (2017).
10. M. D. W. Piper, E. Blanc, R. Leitão-Gonçalves, M. Yang, X. He, N. J. Linford, M. P. Hoddinott, C. Hopfen, G. A. Soultoukis, C. Niemeyer, F. Kerr, S. D. Pletcher, C. Ribeiro, L. Partridge, A holidic medium for *Drosophila melanogaster*. *Nat. Methods* **11**, 100–105 (2013).
11. D. Drummond-Barbosa, A. C. Spradling, Stem cells and their progeny respond to nutritional changes during *Drosophila* oogenesis. *Dev. Biol.* **231**, 265–278 (2001).
12. Y. Shimada, K. M. Burn, R. Niwa, L. Cooley, Reversible response of protein localization and microtubule organization to nutrient stress during *Drosophila* early oogenesis. *Dev. Biol.* **355**, 250–262 (2011).
13. K. J. Min, M. F. Hogan, M. Tatar, D. M. O'Brien, Resource allocation to reproduction and soma in *Drosophila*: A stable isotope analysis of carbon from dietary sugar. *J. Insect Physiol.* **52**, 763–770 (2006).
14. B. Zanco, C. K. Mirth, C. M. Sgrò, M. D. W. Piper, A dietary sterol trade-off determines lifespan responses to dietary restriction in *Drosophila melanogaster* females. *eLife* **10**, e62335 (2021).
15. Z. Carvalho-Santos, R. Cardoso-Figueiredo, A. P. Elias, I. Tastekin, C. Baltazar, C. Ribeiro, Cellular metabolic reprogramming controls sugar appetite in *Drosophila*. *Nat. Metab.* **2**, 958–973 (2020).
16. S. Matsuoka, A. R. Armstrong, L. L. Sampson, K. M. Laws, D. Drummond-Barbosa, Adipocyte metabolic pathways regulated by diet control the female germline stem cell lineage in *Drosophila melanogaster*. *Genetics* **206**, 953–971 (2017).
17. T. Ameku, Y. Yoshinari, M. J. Texada, S. Kondo, K. Amezawa, G. Yoshizaki, Y. Shimada-Niwa, R. Niwa, Midgut-derived neuropeptide F controls germline stem cell proliferation in a mating-dependent manner. *PLOS Biol.* **16**, e2005004 (2018).
18. A. Santel, T. Winhauer, N. Blümer, R. Renkawitz-Pohl, The *Drosophila don juan (dj)* gene encodes a novel sperm specific protein component characterized by an unusual domain of a repetitive amino acid motif. *Mech. Dev.* **64**, 19–30 (1997).
19. Y. Yoshinari, T. Ameku, S. Kondo, H. Tanimoto, T. Kuraishi, Y. Shimada-Niwa, R. Niwa, Neuronal octopamine signaling regulates mating-induced germline stem cell increase in female *Drosophila melanogaster*. *eLife* **9**, e57101 (2020).
20. Y. Yoshinari, H. Kosakamoto, T. Kamiyama, R. Hoshino, R. Matsuoka, S. Kondo, H. Tanimoto, A. Nakamura, F. Obata, R. Niwa, The sugar-responsive enteroendocrine neuropeptide F regulates lipid metabolism through glucagon-like and insulin-like hormones in *Drosophila melanogaster*. *Nat. Commun.* **12**, 4818 (2021).
21. W. Song, J. A. Veenstra, N. Perrimon, Control of lipid metabolism by tachykinin in *Drosophila*. *Cell Rep.* **9**, 40–47 (2014).
22. C. Xie, X. Wang, R. L. Young, M. Horowitz, C. K. Rayner, T. Wu, Role of intestinal bitter sensing in enteroendocrine hormone secretion and metabolic control. *Front. Endocrinol.* **9**, 576 (2018).
23. J. Dyer, K. S. H. Salmon, L. Zibrik, S. P. Shirazi-Beechey, Expression of sweet taste receptors of the T1R family in the intestinal tract and enteroendocrine cells. *Biochem. Soc. Trans.* **33**, 302–305 (2005).
24. J.-H. Park, J. Y. Kwon, Heterogeneous expression of *Drosophila* gustatory receptors in enteroendocrine cells. *PLOS ONE* **6**, e29022 (2011).
25. J. Slone, J. Daniels, H. Amrein, Sugar receptors in *Drosophila*. *Curr. Biol.* **17**, 1809–1816 (2007).
26. S. Fujii, A. Yavuz, J. Slone, C. Jagge, X. Song, H. Amrein, *Drosophila* sugar receptors in sweet taste perception, olfaction, and internal nutrient sensing. *Curr. Biol.* **25**, 621–627 (2015).
27. A. French, M. A. Agha, A. Mitra, A. Yanagawa, M. J. Sellier, F. Marion-Poll, *Drosophila* bitter taste(s). *Front. Integr. Neurosci.* **9**, 58 (2015).
28. S. Chyb, A. Dahanukart, A. Wickens, J. R. Carlson, *Drosophila* Gr5a encodes a taste receptor tuned to trehalose. *Proc. Natl. Acad. Sci. U.S.A.* **100**, 14526–14530 (2003).
29. T. Miyamoto, J. Slone, X. Song, H. Amrein, A fructose receptor functions as a nutrient sensor in the *Drosophila* brain. *Cell* **151**, 1113–1125 (2012).
30. X. Guo, C. Yin, F. Yang, Y. Zhang, H. Huang, J. Wang, B. Deng, T. Cai, Y. Rao, R. Xi, The cellular diversity and transcription factor code of *Drosophila* enteroendocrine cells. *Cell Rep.* **29**, 4172–4185.e5 (2019).
31. K. Sato, K. Tanaka, K. Touhara, Sugar-regulated cation channel formed by an insect gustatory receptor. *Proc. Natl. Acad. Sci. U.S.A.* **108**, 11680–11685 (2011).
32. J. H. Park, J. Chen, S. Jang, T. J. Ahn, K. J. Kang, M. S. Choi, J. Y. Kwon, A subset of enteroendocrine cells is activated by amino acids in the *Drosophila* midgut. *FEBS Lett.* **590**, 493–500 (2016).
33. K. Masuyama, Y. Zhang, Y. Rao, J. W. Wang, Mapping neural circuits with activity-dependent nuclear import of a transcription factor. *J. Neurogenet.* **26**, 89–102 (2012).
34. H. G. Hers, Le mécanisme de la transformation de glucose en fructose par les vésicules séminales. *Biochim. Biophys. Acta* **22**, 202–203 (1956).
35. H. Sano, A. Nakamura, M. Yamane, H. Niwa, T. Nishimura, K. Araki, K. Takemoto, K. Ishiguro, H. Aoki, M. Kojima, The polyol pathway is an evolutionarily conserved system for sensing glucose uptake. *PLoS Biol.* **20**, e3001678 (2022).
36. H. Li, J. Janssens, M. De Waegeneer, S. S. Kolluru, K. Davie, V. Gardeux, W. Saelens, F. P. A. David, M. Brbić, K. Spanier, J. Leskovec, C. N. McLaughlin, Q. Xie, R. C. Jones, K. Brueckner, J. Shim, S. G. Tattikota, F. Schnorrer, K. Rust, T. G. Nystul, Z. Carvalho-Santos, C. Ribeiro, S. Pal, S. Mahadevaraju, T. M. Przytycka, A. M. Allen, S. F. Goodwin, C. W. Berry, M. T. Fuller, H. White-Cooper, E. L. Matunis, S. D. Nardo, A. Galenza, L. E. O'Brien, J. A. T. Dow, FCA Consortium, H. Jasper, B. Oliver, N. Perrimon, B. Deplancke, S. R. Quake, L. Luo, S. Aerts, D. Agarwal, Y. Ahmed-Braimah, M. Arbeitman, M. M. Ariss, J. Augsburg, K. Ayush, C. C. Baker, T. Banisch, K. Birker, R. Bodmer, B. Bolival, S. E. Brantley, J. A. Brill, N. C. Brown, N. A. Buehner, X. T. Cai, R. Cardoso-Figueiredo, F. Casares, A. Chang, T. R. Clandinin, S. Crasta, C. Desplan, A. M. Detweiler, D. B. Dhakan, E. Donà, S. Engert, S. Floc'hlay, N. George, A. J. González-Segarra, A. K. Groves, S. Gumbin, Y. Guo, D. E. Harris, Y. Heifetz, S. L. Holtz, F. Horns, B. Hudry, R.-J. Hung, Y. N. Jan, J. S. Jaszczak, G. S. X. E. Jefferis, J. Karkianis, T. L. Karr, N. S. Katheder, J. Kezos, A. A. Kim, S. K. Kim, L. Kockel, N. Konstantinides, T. B. Kornberg, H. M. Krause, A. T. Labott, M. Laturney, R. Lehmann, S. Leinwand, J. Li, J. S. S. Li, K. Li, K. Li, L. Li, T. Li, M. Litovchenko, H.-H. Liu, Y. Liu, T.-C. Lu, J. Manning, A. Mase, M. Matera-Vatnick, N. R. Matias, C. E. McDonough-Goldstein, A. M. Geever, A. D. McLachlan, P. Moreno-Roman, N. Neff, M. Neville, S. Ngo, T. Nielsen, C. E. O'Brien, D. Osumi-Sutherland, M. A. Int. D. I. Papatheodorou, M. Petkovic, C. Pilgrim, A. O. Pisco, C. Reisenman, E. N. Sanders, G. D. Santos, K. Scott, A. Sherlekar, P. Shiu, D. Sims, R. V. Sit, M. Slaidina, H. E. Smith, G. Sterne, Y.-H. Su, D. Sutton, M. Tamayo, M. Tan, I. Tastekin, C. Treiber, D. Vacek, G. Vogler, S. Waddell, W. Wang, R. I. Wilson, M. F. Wolfner, Y.-C. E. Wong, A. Xie, J. Xu, S. Yamamoto, J. Yan, Z. Yao, K. Yoda, R. Zhu, R. P. Zinzen, Fly Cell Atlas: A single-nucleus transcriptomic atlas of the adult fruit fly. *Science* **375**, eabk2432 (2022).
37. M. T. Le, R. F. Frye, C. J. Rivard, J. Cheng, K. K. McFann, M. S. Segal, R. J. Johnson, J. A. Johnson, Effects of high-fructose corn syrup and sucrose on the pharmacokinetics of fructose and acute metabolic and hemodynamic responses in healthy subjects. *Metabolism* **61**, 641–651 (2012).
38. P. Y. Musso, P. Junca, M. D. Gordon, A neural circuit linking two sugar sensors regulates satiety-dependent fructose drive in *Drosophila*. *Sci. Adv.* **7**, 186 (2021).
39. L. Yan, C. Liang-jun Yan, Redox imbalance stress in diabetes mellitus: Role of the polyol pathway. *Animal Model Exp. Med.* **1**, 7–13 (2018).
40. U.S. Department of Agriculture, FoodData Central (2022); <https://fdc.nal.usda.gov/>.
41. J. Jaenike, Induction of host preference in *Drosophila melanogaster*. *Oecologia* **58**, 320–325 (1983).
42. R. E. Kuhre, F. M. Gribble, B. Hartmann, F. Reimann, J. A. Windeløv, J. F. Rehfeld, J. J. Holst, Fructose stimulates GLP-1 but not GIP secretion in mice, rats, and humans. *Am. J. Physiol. Gastrointest. Liver Physiol.* **306**, 622–630 (2014).
43. F. A. Duca, T. M. Z. Waise, W. T. Peppler, T. K. T. Lam, The metabolic impact of small intestinal nutrient sensing. *Nat. Commun.* **12**, 903 (2021).

44. A. Malita, O. Kubrak, T. Koyama, N. Ahrentlöv, M. J. Texada, S. Nagy, K. V. Halberg, K. Rewitz, A gut-derived hormone suppresses sugar appetite and regulates food choice in *Drosophila*. *Nat. Metab.* **4**, 1532–1550 (2022).
45. A. A. Gupte, H. J. Pownall, D. J. Hamilton, Estrogen: An emerging regulator of insulin action and mitochondrial function. *J. Diabetes Res.* **2015**, 916585 (2015).
46. J. B. Josimovich, B. L. Atwood, D. A. Goss, Luteotrophic, immunologic and electrophoretic properties of human placental lactogen. *Endocrinology* **73**, 410–420 (1963).
47. T. Wada, S. Hori, M. Sugiyama, E. Fujisawa, T. Nakano, H. Tsuneki, K. Nagira, S. Saito, T. Sasaoka, Progesterone inhibits glucose uptake by affecting diverse steps of insulin signaling in 3T3-L1 adipocytes. *Am. J. Physiol. Endocrinol. Metabol.* **298**, E881–E888 (2010).
48. A. Scalfani, Sweet taste signaling in the gut. *Proc. Natl. Acad. Sci. U.S.A.* **104**, 14887–14888 (2007).
49. R. F. Margolskee, J. Dyer, Z. Kokrashvili, K. S. H. Salmon, E. Illegems, K. Daly, E. L. Maillet, Y. Ninomiya, B. Mosinger, S. P. Shirazi-Beechey, T1R3 and gustducin in gut sense sugars to regulate expression of Na⁺-glucose cotransporter 1. *Proc. Natl. Acad. Sci. U.S.A.* **104**, 15075–15080 (2007).
50. G. E. DuBois, Molecular mechanism of sweetness sensation. *Physiol. Behav.* **164**, 453–463 (2016).
51. T. R. Regnault, S. Gentili, O. Sarr, C. R. Toop, D. M. Sloboda, Fructose, pregnancy and later life impacts. *Clin. Exp. Pharmacol. Physiol.* **40**, 824–837 (2013).
52. M. D. Thompson, B. J. Debosch, Maternal fructose diet-induced developmental programming. *Nutrients* **13**, 3278 (2021).
53. B. Deng, Q. Li, X. Liu, Y. Cao, B. Li, Y. Qian, R. Xu, R. Mao, E. Zhou, W. Zhang, J. Huang, Y. Rao, Chemoconnectomics: Mapping chemical transmission in *Drosophila*. *Neuron* **101**, 876–893.e4 (2019).
54. A. Jenett, G. M. Rubin, T. T. B. Ngo, D. Shepherd, C. Murphy, H. Dionne, B. D. Pfeiffer, A. Cavallaro, D. Hall, J. Jeter, N. Iyer, D. Fetter, J. H. Hausenfluck, H. Peng, E. T. Trautman, R. R. Svirskas, E. W. Myers, Z. R. Iwinski, Y. Aso, G. M. DePasquale, A. Enos, P. Hulamm, S. C. B. Lam, H. H. Li, T. R. Laverty, F. Long, L. Qu, S. D. Murphy, K. Rokicki, T. Safford, K. Shaw, J. H. Simpson, A. Sowell, S. Tae, Y. Yu, C. T. Zugates, A GAL4-driver line resource for *Drosophila* neurobiology. *Cell Rep.* **2**, 991–1001 (2012).
55. J. R. Kennerdell, R. W. Carthew, Heritable gene silencing in *Drosophila* using double-stranded RNA. *Nat. Biotechnol.* **18**, 896–898 (2000).
56. L. A. Weiss, A. Dahanukar, J. Y. Kwon, D. Banerjee, J. R. Carlson, The molecular and cellular basis of bitter taste in *Drosophila*. *Neuron* **69**, 258–272 (2011).
57. L. A. Perkins, L. Holderbaum, R. Tao, Y. Hu, R. Sopko, K. McCall, D. Yang-Zhou, I. Flockhart, R. Binari, H. S. Shim, A. Miller, A. Housden, M. Foss, S. Randkelv, C. Kelley, P. Namgyal, C. Villalta, L. P. Liu, X. Jiang, Q. Huan-Huan, X. Wang, A. Fujiyama, A. Toyoda, K. Ayers, A. Blum, B. Czech, R. Neumuller, D. Yan, A. Cavallaro, K. Hibbard, D. Hall, L. Cooley, G. J. Hannon, R. Lehmann, A. Parks, S. E. Mohr, R. Ueda, S. Kondo, J. Q. Ni, N. Perrimon, The transgenic RNAi project at Harvard medical school: Resources and validation. *Genetics* **201**, 843–852 (2015).
58. E. T. Ables, D. Drummond-Barbosa, The steroid hormone ecdysone functions with intrinsic chromatin remodeling factors to control female germline stem cells in *Drosophila*. *Cell Stem Cell* **7**, 581–592 (2010).
59. T. Nishimura, Feedforward regulation of glucose metabolism by steroid hormones drives a developmental transition in *Drosophila*. *Curr. Biol.* **30**, 3624–3632.e5 (2020).
60. T. Yamada, K.-I. Hironaka, O. Habara, Y. Morishita, T. Nishimura, A developmental checkpoint directs metabolic remodelling as a strategy against starvation in *Drosophila*. *Nat. Metab.* **2**, 1096–1112 (2020).
61. Z. Pang, J. Chong, G. Zhou, D. A. de Lima Morais, L. Chang, M. Barrette, C. Gauthier, P. É. Jacques, S. Li, J. Xia, MetaboAnalyst 5.0: Narrowing the gap between raw spectra and functional insights. *Nucleic Acids Res.* **49**, W388–W396 (2021).
62. R. Matsushita, T. Nishimura, Trehalose metabolism confers developmental robustness and stability in *Drosophila* by regulating glucose homeostasis. *Commun. Biol.* **3**, 170 (2020).
63. W. W. Ja, G. B. Carvalho, E. M. Mak, N. N. de La Rosa, A. Y. Fang, J. C. Liang, T. Brummel, S. Benzer, Prandiology of *Drosophila* and the CAFE assay. *Proc. Natl. Acad. Sci. U.S.A.* **104**, 8253–8256 (2007).
64. J. M. Tennesen, W. E. Barry, J. Cox, C. S. Thummel, Methods for studying metabolism in *Drosophila*. *Methods* **68**, 105–115 (2014).

Acknowledgments: We thank H. Amrein, J. R. Carlson, J. Y. Kwon, M. Miura, C. Miyamoto, Bloomington *Drosophila* Stock Center, Vienna *Drosophila* Resource Center, and Developmental Studies Hybridoma Bank for providing us with fly stocks and other reagents. We are also grateful to S.-F. Wu for advice on this study and S. D. Aird for editing the manuscript. R.H. and Y.Y. were recipients of fellowships from the Japan Society for the Promotion of Science.

Funding: This study was funded by the Ministry of Education, Culture, Sports, Science and Technology of Japan, Grant-in-Aid for Scientific Research on Innovative Areas 19H05240 (R.N.); the Ministry of Education, Culture, Sports, Science and Technology of Japan, Grant-in-Aid for Scientific Research on Innovative Areas 21H00226 (R.N.); Japan Society for the Promotion of Science KAKENHI grant 22H00414 (R.N.); Japan Society for the Promotion of Science KAKENHI grant 21 J20279 (R.H.); Japan Society for the Promotion of Science KAKENHI grant 20 K06647 (H.S.); Japan Society for the Promotion of Science KAKENHI grant 22H05638 (H.S.); Japan Agency for Medical Research and Development AMED-CREST grant 20gm1110001s0304 (R.N.); Japan Agency for Medical Research and Development AMED-CREST grant 21gm1110001s0305 (R.N.); Japan Agency for Medical Research and Development AMED-CREST grant 22gm1110001s0306 (R.N.); and the joint research program of the Institute for Molecular and Cellular Regulation, Gunma University 21020 (R.N.). **Author contributions:** Conceptualization: R.H. and R.N. Methodology: R.H., H.S., Y.Y., T.N., and R.N. Investigation: R.H., H.S., Y.Y., T.N., and R.N. Visualization: R.H. and T.N. Supervision: R.N. Writing—original draft: R.H. and R.N. Writing—review and editing: R.H., H.S., Y.Y., T.N., and R.N. **Competing interests:** The authors declare that they have no competing interests. **Data and materials availability:** All data needed to evaluate the conclusions in the paper are present in the paper and/or the Supplementary Materials.

Submitted 23 June 2022

Accepted 20 January 2023

Published 24 February 2023

10.1126/sciadv.add5551